Received: 15 April 2020 | Revised: 14 September 2020 | Accepted: 15 September 2020

DOI: 10.1002/cne.25037

RESEARCH ARTICLE

JCN RESEARCH IN SYSTEMS NEUROSCIENCE THE JOURNAL OF COMPARATIVE NEUROLOGY WILEY

Aversive teaching signals from individual dopamine neurons in larval *Drosophila* show qualitative differences in their temporal "fingerprint"

Aliće Weiglein[1] | Juliane Thoener[1] | Irina Feldbruegge[1] | Louisa Warzog[1] | Nino Mancini[1] | Michael Schleyer[1] | Bertram Gerber[1,2,3]

[1]Department of Genetics, Leibniz Institute for Neurobiology, Magdeburg, Germany

[2]Institute of Biology, Otto von Guericke University Magdeburg, Germany

[3]Center for Behavioral Brain Sciences, Otto von Guericke University, Magdeburg, Germany

Correspondence
Aliće Weiglein, Institute of Anatomy, Otto von Guericke University Magdeburg, Germany, and Bertram Gerber, Department of Genetics, Leibniz Institute for Neurobiology, Magdeburg, Germany.
Email: alice.weiglein@med.ovgu.de (A. W.); bertram.gerber@lin-magdeburg.de (B. G.)

Funding information
Deutsche Forschungsgemeinschaft, Grant/Award Numbers: CRC 779 Motivated Behavior, FOR 2705 Mushroom body, GE 1091/4-1; German-Israeli Foundation for Science, Grant/Award Number: G-2502-418.13/2018

[Correction added on 25 January 2021, after first online publication: Projekt Deal funding statement has been added.]

Abstract

Dopamine serves many functions, and dopamine neurons are correspondingly diverse. We use a combination of optogenetics, behavioral experiments, and high-resolution video-tracking to probe for the functional capacities of two single, identified dopamine neurons in larval *Drosophila*. The DAN-f1 and the DAN-d1 neuron were recently found to carry aversive teaching signals during Pavlovian olfactory learning. We enquire into a fundamental feature of these teaching signals, namely their temporal "fingerprint". That is, receiving punishment feels bad, whereas being relieved from it feels good, and animals and humans alike learn with opposite valence about the occurrence and the termination of punishment (the same principle applies in the appetitive domain, with opposite sign). We find that DAN-f1 but not DAN-d1 can mediate such timing-dependent valence reversal: presenting an odor before DAN-f1 activation leads to learned avoidance of the odor (punishment memory), whereas presenting the odor upon termination of DAN-f1 activation leads to learned approach (relief memory). In contrast, DAN-d1 confers punishment memory only. These effects are further characterized in terms of the impact of the duration of optogenetic activation, the temporal stability of the memories thus established, and the specific microbehavioral patterns of locomotion through which they are expressed. Together with recent findings in the appetitive domain and from adult *Drosophila*, our results suggest that heterogeneity in the temporal fingerprint of teaching signals might be a more general principle of reinforcement processing through dopamine neurons.

KEYWORDS

Associative learning, optogenetics, punishment, relief, research resource identifiers (RRIDs), timing-dependent valence reversal

1 | INTRODUCTION

Avoiding punishment can be a powerful goal of behavior. Accordingly, animals and humans alike are able to learn predictors of the occurrence of punishment, a process that has been studied in detail across species. It is less widely acknowledged, however, that learning can also take place from the termination of punishment. Indeed, delivering versus terminating punishment can induce affect of opposite valence. It feels bad to receive punishment but it feels good to be relieved from it (Solomon & Corbit, 1974) (Figure 1a), resulting in aversive and

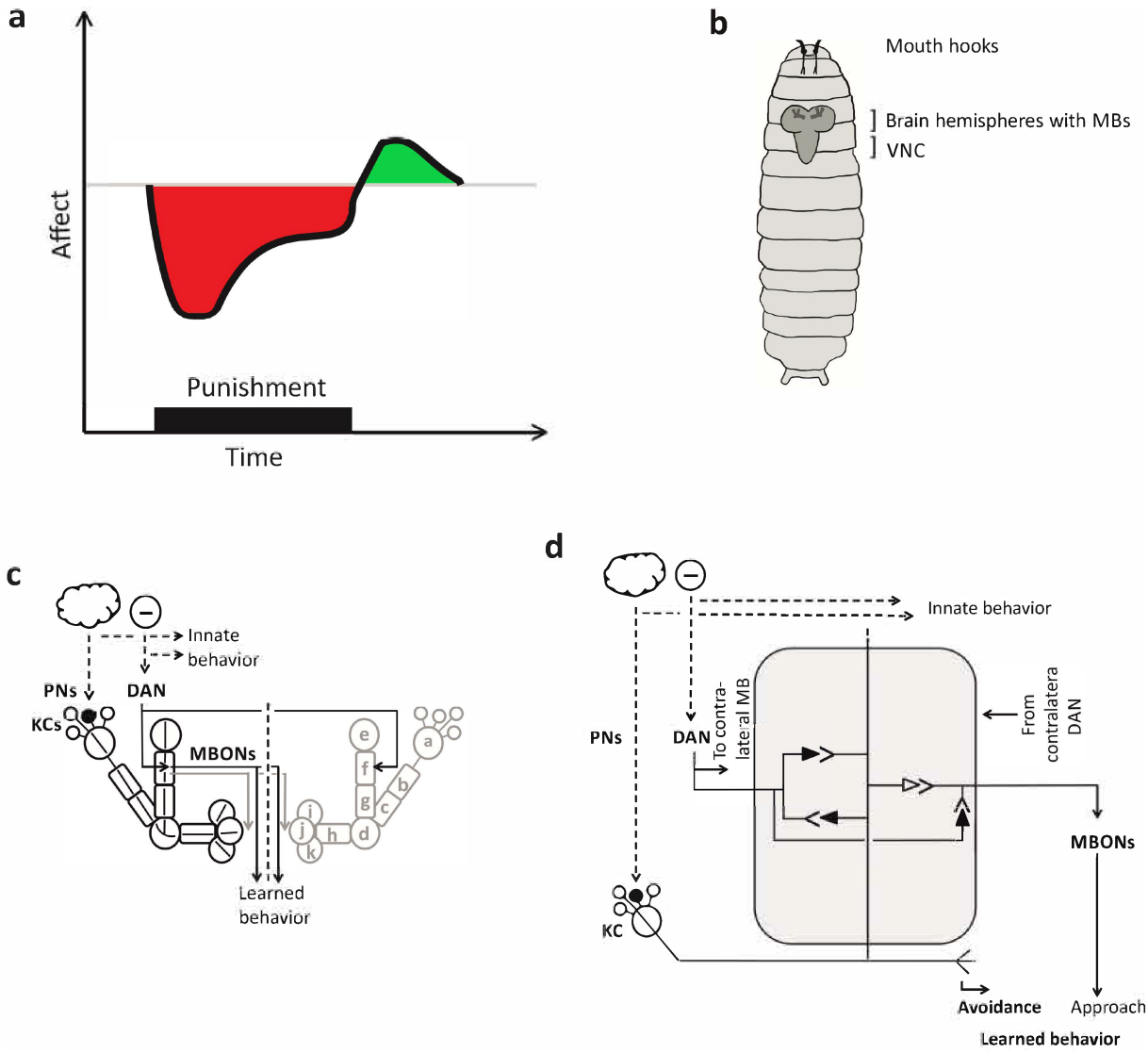

FIGURE 1 Affect dynamics as well as topology and connectivity of the larval learning and memory center. (a) Schematic of the time course of affect upon receiving a negative stimulus such as punishment. Initially negative affect (red) dominates, followed upon termination by less intense positive affect (green) (after Solomon & Corbit, 1974). (b) Sketch of a *Drosophila* third instar larva showing its body, the mouth hooks, brain hemispheres and mushroom bodies (MBs, white), and the ventral nerve cord (VNC). (c) Schematic of the compartmental arrangement of the mushroom bodies. Letters a-k indicate compartment identity. As shown for the f-compartment as an example, at the mushroom body intrinsic Kenyon cells (KCs) a coincidence of signals from olfactory projection neurons (PNs) and intersecting teaching signals from dopaminergic neurons (DANs) can be detected. Such a coincidence can lead to a change in the connection from the subset of KCs in which the coincidence was detected onto the mushroom body output neurons (MBONs). The f-compartment gives rise to two MBONs, MBON-f1 and MBON-f2. Both DAN-f1 and these MBONs receive input only ipsilateral to their cell bodies, yet provide output towards both hemispheres. (d) "Canonical" within-compartment connectivity, for the f-compartment as an example. Filled triangles represent presynapses, forked lines postsynapses. The open triangle indicates experience-dependent depression of the respective presynapse. If the KC-MBON synapse of an approach-promoting MBON is depressed, the activity of avoidance-promoting MBONs from other compartments will prevail, leading to net learned avoidance. For more details and references, see Introduction [Color figure can be viewed at wileyonlinelibrary.com]

appetitive learning, respectively, of the associated cues. Such learning is observed in animals as well as humans and is referred to as timing-dependent valence reversal (reviewed in Gerber et al., 2014, Navratilova, Atcherley, & Porreca, 2015, Gerber et al., 2019). The same dichotomy applies for reward processing, with opposite sign (Hellstern, Malaka, & Hammer, 1998). Timing-dependent valence reversal features prominently in many computational models of reinforcement learning (overview in Malaka, 1999) and is arguably essential for adapting to the causal event-structure of the world. Here, we investigate timing-dependent valence reversal in the larvae of the fruit fly *Drosophila melanogaster* as mediated by two identified dopamine neurons recently found to confer teaching signals for associative learning in the aversive domain (Eschbach et al., 2020a).

Drosophila is a suitable model system for such an endeavor because it combines convenient experimental tractability by means of genetic manipulation, robust behavioral paradigms for associative learning, a high degree of similarity to humans at the molecular level, and a numerically simple brain. The learning of associations between odor and electric shock punishment has been studied in particular detail in adult flies (Aso & Rubin, 2020; Boto, Stahl, & Tomchik, 2020; Cognigni, Felsenberg, & Waddell, 2018; Heisenberg, 2003; McGuire, Deshazer, & Davis, 2005). In brief, this association process takes place in the Kenyon cells (KCs) of the mushroom body, a third-order brain structure in the insects providing a combinatorial, specific, and sparse representation of the environment, including odors. Along their elongated axonal fibers, the KCs also receive intersecting input from mostly dopaminergic neurons (DANs) that can be broadly classified as mediating modulatory teaching signals concerning either punishment or reward. The coincidence of the activation of DANs and the specific set of KCs representing the odor can lead to presynaptic plasticity at the synapse from the KCs to mushroom body output neurons (MBONs). These MBONs can be broadly categorized as either approach- or avoidance promoting. DANs and MBONs overlap in a regionally confined way along the KC fibers, establishing a characteristic compartmental organization. Typically, punishment-DANs are matched up with approach-promoting MBONs, and reward-DANs with avoidance-promoting MBONs. Upon odor-shock coincidence, synaptic strength between the odor-activated KCs and approach-promoting MBONs is reduced, such that for a punished odor the balance between approach and avoidance is shifted in favor of avoidance. A similar organization, in separate mushroom body compartments and their respective DANs and MBONs, underlies reward learning, and likely the learning about punishment and reward in larval *Drosophila* as well (Gerber & Stocker, 2007; Eschbach et al., 2020a; Eschbach et al., 2020b; Thum & Gerber 2019) **(**Figure 1b-d**)**.

Using the association of odor with electric shock punishment in adult *Drosophila*, timing-dependent valence reversal was reported by Tanimoto, Heisenberg, & Gerber (2004) and subsequently analyzed in some detail (Yarali et al., 2008; Yarali et al., 2009; Yarali & Gerber, 2010; Diegelmann et al., 2013; Niewalda et al., 2015; Appel et al., 2016; also see Vogt, Yarali, & Tanimoto, 2015). Strikingly, timing-dependent valence reversal was also found for the optogenetic activation of the DAN known as PPL1-01 (Aso & Rubin, 2016; König et al., 2018; Aso & Rubin, 2020; for a broader set of DANs: Handler et al., 2019). Other DANs also confer aversive teaching signals but with different "temporal fingerprints" and no—or at least no robust—timing-dependent valence reversal (Aso & Rubin, 2016; König et al., 2018). We ask whether such qualitative differences among punishment DANs in the temporal fingerprint of their teaching signals are found in larval *Drosophila* as well, suggesting heterogeneity in DAN function as a general principle.

Larval *Drosophila* are an emerging study case for learning and memory, sharing the above-mentioned experimental advantages of adult flies—yet at about 10-fold lower cell numbers (reviewed in Gerber & Stocker, 2007; Thum & Gerber 2019). Thanks to this numerical simplicity, a complete light microscopy atlas of its neurons and their chemical-synapse connectome is within reach (Gerhard, Andrade, Fetter, Cardona, & Schneider-Mizell, 2017; Li et al., 2014). In particular, all KCs and their pre- and postsynaptic partners have been reconstructed (Eichler et al., 2017; Saumweber et al., 2018; also see Selcho, Pauls, Han, Stocker, & Thum, 2009; Pauls, Selcho, Gendre, Stocker, & Thum, 2010, Rohwedder et al. 2016). Likewise, all pre- and postsynaptic partners of the DANs innervating the mushroom body have been uncovered (Eschbach et al., 2020a; also see Eschbach et al., 2020b). For a subset of these DANs, transgenic drivers for studying their individual behavioral function are available. It has turned out that optogenetic activation of either of two of them can confer a rewarding effect (DAN-i1, DAN-h1; Saumweber et al., 2018), whereas at least two other DANs can be punishing (DAN-f1, DAN-d1 and possibly also DAN-g1; Eschbach et al., 2020a) (regarding broader sets of neurons see Almeida-Carvalho et al., 2017; Eichler et al., 2017; Rohwedder et al., 2016; Schroll et al., 2006). In the appetitive domain, Saumweber et al. (2018) showed that the DAN-i1 teaching signal can confer timing-dependent valence reversal, whereas DAN-h1 has not yet been tested in this regard. Here, we focus on the aversive domain and ask whether the teaching signals from the respective DANs can establish timing-dependent valence reversal.

2 | MATERIALS AND METHODS

This study uses an established protocol for olfactory associative learning with teaching signals from the optogenetic activation of individual dopaminergic mushroom body input neurons (DANs) instead of a real reward or punishment (Saumweber et al., 2018). In brief, one group of larvae receives an odor together with the optogenetic activation of a DAN (paired), whereas a second group receives the odor separate from DAN activation (unpaired). Since odor presentation and DAN activation are relatively short, and because in the paired condition the relative timing of odor and DAN activation is the key experimental variable throughout this study, the present protocol is called "timed protocol". Specifically, in the paired cases the odor is either presented *before* DAN activation (*forward* conditioning: odor-DAN), or *after* DAN activation (*backward* conditioning: DAN-odor) at the intervals specified below. In all cases, a final test determines the level of odor preference in paired-trained versus unpaired-trained larvae.

We note that in Pavlovian terminology, the odor is the conditioned stimulus (CS), DAN activation the unconditioned stimulus (US), and the difference in odor preference between paired-trained versus unpaired-trained larvae our measure of the conditioned response (CR).

2.1 | Animals

We used 5-day-old, third instar, feeding-stage larvae throughout the experiments. Animals were raised on standard food and maintained at 25°C, 60%–70% relative humidity and a 12/12 hr light/dark cycle. Cohorts of approximately 30 larvae were collected from the food vials, rinsed in water, collected in a water droplet and subsequently

used in the respective experiment. In order to investigate the effect of DAN activation, we crossed animals of the effector strain UAS-ChR2-XXL (Bloomington Stock Center no. 58374, RRID: BDSC_58,374; Dawydow et al., 2014) to one of the following Gal4 driver strains, namely SS02180-Gal4, reliably covering the DAN-f1 neuron, or MB328b-Gal4, reliably covering the DAN-d1 neuron, or SS01716-Gal4, reliably covering the DAN-g1 neuron (RRIDs: N/A; all driver strains kindly provided by HHMI Janelia Research Campus). In the offspring of these crosses, the respective DAN can be activated by blue light. All three DANs have previously been shown to mediate punishment (Eschbach et al., 2020a). The expression pattern of all driver strains used in this study was assessed by immunohistochemistry, using either the same UAS-ChR2-XXL effector strain, or 10xUAS-IVS-mCD8::GFP (RRID: N/A; kindly provided by HHMI Janelia Research Campus). To visualize pre−/postsynaptic regions of DAN-f1 and DAN-d1, a UAS-Dsyd-1::GFP/UAS-DenMark double effector strain was used (RRID: N/A; kindly provided by Andreas S. Thum, U Leipzig).

As the driver control, the respective driver strain was crossed to our local copy of w^{1118} (Bloomington Stock Center no. 3605, 5,905, 6,326, RRID: BDSC_3605). We obtained the effector control by crossing the UAS-ChR2-XXL strain to flies carrying both landing sites used for the split-GAL4 (attP40/attP2) but lacking an inserted GAL4 domain (RRID: N/A; kindly provided by HHMI Janelia Research Campus; Pfeiffer et al., 2010). To prevent ChR2-XXL from being activated by ambient room light, the animals were raised in food vials wrapped in black cardboard.

2.2 | The timed protocol for associative learning

Optogenetic experiments were performed inside a custom-made box, within which a light table was equipped with 24 × 12 LEDs with a peak wavelength of 470 nm (Solarox, Dessau-Roßlau, Germany), with a 6-mm-thick diffusion plate of frosted plexiglass on top to ensure uniform light conditions and intensity (120 μW/cm^2). The box was equipped with a black curtain to minimize disturbance by ambient room light. For the learning assay, Petri dishes were placed on top of the diffusion plate surrounded by a ring of 30 infrared LEDs (850 nm; Solarox, Dessau-Roßlau, Germany) behind a polyethylene diffusion ring that provided illumination. Cohorts of approximately 30 larvae were placed at the center of a Petri dish (9 cm inner diameter; Sarstedt, Nümbrecht, Germany) filled with 1% agarose solution (electrophoresis grade; CAS: 9012-36-6, Roth, Karlsruhe, Germany) and subsequently transferred to inside the custom-made box. One training trial lasted 8 min, during which time the larvae stayed on the same Petri dish and the Petri dish lid alone was exchanged either with a lid equipped with four odor-loaded sticky filter papers (*n*-amylacetate; CAS: 628–63-7, Merck, Darmstadt, Germany, diluted 1:20 in paraffin oil; CAS: 8042-47-5, AppliChem, Darmstadt, Germany) or a "mock control", with four sticky filter papers loaded with paraffin. Paraffin has been shown not to have behavioral significance as an odor (Saumweber, Husse, & Gerber, 2011). Three training trials were performed, unless mentioned otherwise. Larvae that crawled onto the lid during training were excluded from the experiments.

Following established protocols (Michels et al., 2017; Saumweber et al., 2011; Saumweber et al., 2018), the larvae were either trained to associate the odor with the optogenetic activation of the respective DAN (paired), or they received odor and DAN activation separately (unpaired). Both odor presentation and DAN activation lasted 30 s, unless mentioned otherwise. Critically, in the paired case the larvae received odor presentation and DAN activation at different relative timings (the inter-stimulus-interval, ISI, defined as the time interval from the onset of odor presentation to the onset of DAN activation). As an example of paired training for an ISI of −10 s (forward conditioning), the animals were placed on a Petri dish and after 1 min 50 s they were presented with the odor for 30 s (Figure 2a, top). DAN activation started at minute 2 by turning on the blue light, i.e. 10 s after the onset of the odor (ISI -10 s), and lasted for 30 s, too. After the end of the DAN activation an additional 3.5 min were allowed to pass, before at minute 6 a 30-s presentation of paraffin as the odor-solvent followed to equate handling with the unpaired group. Then the larvae were left untreated until minute 8, when the clock was reset and the next training trial was started. Of note is that the sequence of events during the training trials, i.e. presentation of paraffin or of odor with DAN activation, was reversed in half of the cases. For each group paired-trained with a given ISI, an unpaired group was run. In this case odor was presented after 2 min and paraffin as the solvent after 5:50 min with DAN activation starting after 6 min (Figure 2a, bottom). Again, the sequence of these events was reversed in half of the cases. An example for training with an ISI of 60 s (backward conditioning) is shown in Figure 2b.

After such training, the larvae were transferred to a test Petri dish, also filled with 1% agarose. The testing lid was equipped with two filter papers on opposite sides; one was loaded with the odor, the other with paraffin. The test was carried out in the presence of the blue light; this was done because punishment-related learned behavior is a form of learned escape which is facilitated under aversive conditions (Gerber & Hendel, 2006; Schleyer et al., 2011). After 3 min, the number of larvae (#) on the odor side, on the paraffin side, and in a 10-mm-wide middle zone was counted. Larvae on the lid were excluded from the analysis, whereas larvae crawling up the side-walls of the Petri dish were counted for the respective side. A preference index (PREF) was calculated as follows, separately for the paired-trained and the unpaired-trained animals:

$$PREF = \frac{(\#\text{Odor} - \#\text{Paraffin})}{\#\text{Total}} \quad (1)$$

Preference indices may range from +1 to −1, with positive values indicating preference and negative values indicating avoidance of the

odor. From the PREF scores after paired and unpaired training, a performance index (PI) was calculated:

$$PI = \frac{(\text{PREF } Paired - \text{PREF } Unpaired)}{2} \quad (2)$$

Performance indices may range from +1 to −1. Positive PIs indicate appetitive associative memory, whereas negative values indicate aversive associative memory.

In cases of genetic controls being trained and tested along with the experimental genotype, vials were coded and the experimenters were thus blind to genotype.

2.3 | Microbehavioral effects of associative memories

The behavior of larvae during the test situation was video-tracked and analyzed as described in detail in Paisios, Rjosk, Pamir, & Schleyer (2017). In general, larvae alternately perform relatively straight forward locomotion, called runs, and lateral head movements, called head casts (HC), which are often followed by changes in direction. This leads to the typical zig-zagging pattern of the locomotion of larvae on a Petri dish surface (Gershow et al., 2012; Gomez-Marin & Louis, 2014; Gomez-Marin, Stephens, & Louis, 2011). Here, an HC was detected whenever the angular velocity of a vector through the animal's head exceeded a threshold of 35 °/s and ended as soon as that angular velocity dropped below that threshold again. If the angular velocity of a vector through the animal's tail at the same time exceeded a threshold of 45 °/s (a somewhat "funny" walk, happening very rarely), this event was not counted as an HC. In accordance with previous studies, only HCs with an HC angle >20° were taken into account (Paisios, Rjosk, Pamir, & Schleyer 2017; Schleyer et al., 2015; Thane, Viswanathan, Meyer, Paisios, & Schleyer, 2019). The time when an animal was not head-casting was regarded as a run, omitting 1.5 seconds before and after an HC to exclude the decelerating and accelerating phases that usually happen before and after an HC, respectively.

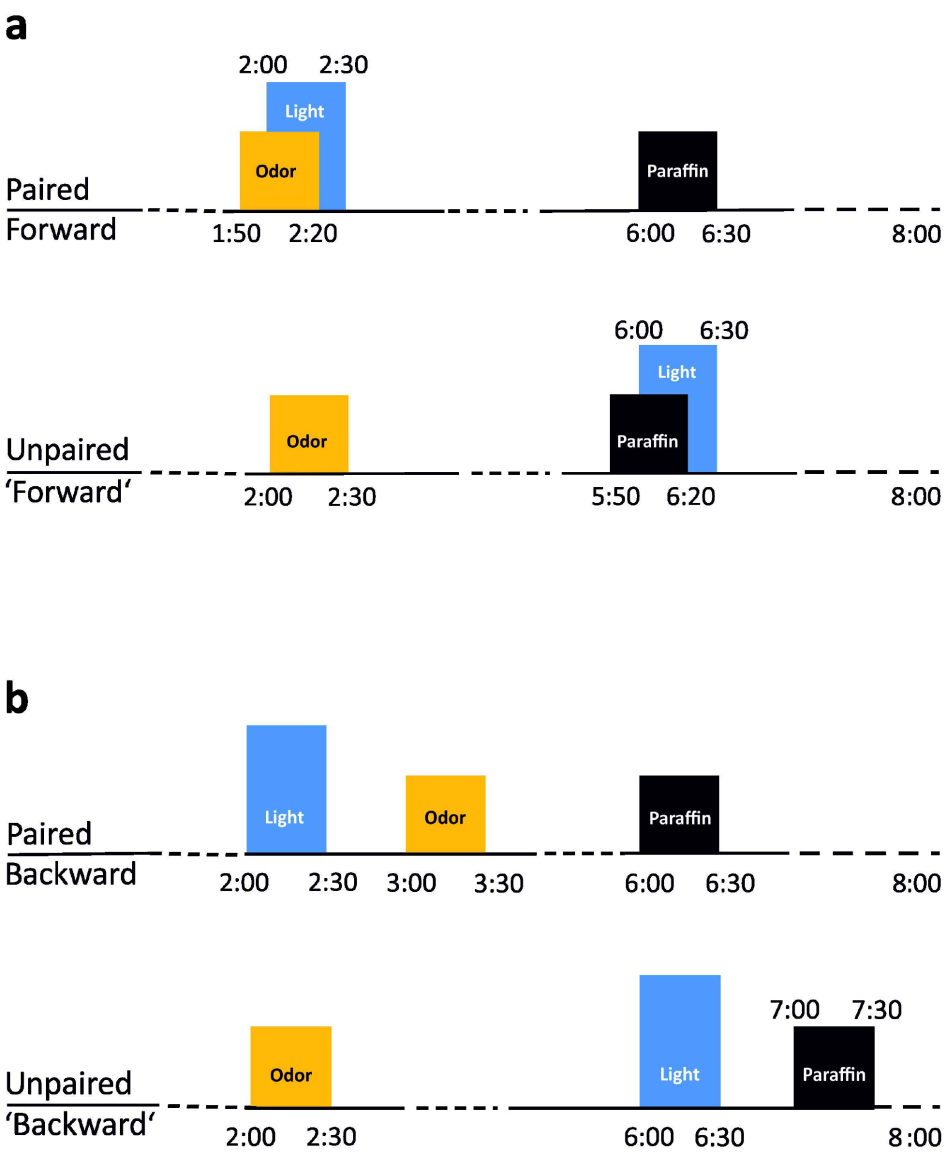

FIGURE 2 Training procedure. Larvae were trained to associate the odor with the optogenetic activation of the respective DAN (paired), or received odor and DAN activation separately (unpaired). Both odor presentation and DAN activation lasted 30 s. In the paired case larvae received odor presentation and DAN activation at different relative timings (inter-stimulus-interval, ISI, defined as the time interval from the onset of DAN activation to the onset of odor presentation). (a) Example time-lines for forward conditioning at an ISI of −10 s with the paired presentation (odor-DAN activation) followed by presentation of paraffin as the solvent (top row), and for different groups of larvae for unpaired training (bottom row). Notably, the sequence of events during the training trials, i.e. odor-DAN activation and paraffin presentation for the paired case, or odor presentation and paraffin-DAN activation for the unpaired case, was reversed in half of the cases. (b) As in (a), for backward conditioning at an ISI of 60 s. Yellow rectangles indicate the odor n-amylacetate, black rectangles paraffin as the solvent, and blue rectangles optogenetic DAN activation. Unless mentioned otherwise, three such 8-min training trials were performed, followed by a test for odor preference [Color figure can be viewed at wileyonlinelibrary.com]

Three aspects of these behaviors were analyzed. The first refers to the run speed, i.e. to the average speed (mm/s) of the larval midpoint during runs. The modulation of run speed was calculated as:

$$\text{Run speed} - \text{modulation} = \frac{\textit{Run speed towards} - \textit{Run speed away}}{\textit{Run speed towards} + \textit{Run speed away}} \quad (3)$$

Thus, if animals modified their run speed such that they speeded up whenever they headed away from the odor and slowed down whenever they headed towards an odor, we would obtain a negative Run speed-modulation, indicating odor aversion. To judge the impact of associative memory on run speed, these measures were compared between paired-trained and unpaired-trained animals.

The second aspect of chemotactic locomotion refers to the rate of HCs (HCs per second, HC/s). The modulation of HC rate was calculated as follows:

$$\textit{HC rate} - \textit{modulation} = \frac{\#\text{HC/s (away)} - \#\text{HC/s (towards)}}{\#\text{HC/s (away)} + \#\text{HC/s (towards)}} \quad (4)$$

Positive scores thus mean that larvae perform more head casts while moving away from the odor than while moving towards it, which would indicate odor attraction. By contrast, negative scores would indicate odor aversion. Again, to judge the impact of associative memory on HCs, these measures were compared between paired-trained and unpaired-trained animals.

The third aspect investigated was the modulation of HC direction, which is measured by the reorientation per HC:

$$\textit{Reorientation per HC} = \text{abs before HC} - \text{abs after HC} \quad (5)$$

The absolute heading angle (abs) indicates how the head of the larva is oriented relative to the odor. Thus, at absolute heading angles of 0° or 180° the odor would be to the front or rear of the larva, respectively. Positive scores occur when the head cast directs the larva towards the odor, indicating attraction. Again, negative scores indicate aversion, and comparisons between paired- and unpaired-trained animals were used to determine the impact of associative memory.

2.4 | Immunohistochemistry

Whole mounts of larval brains of the respective experimental genotype were prepared to assess ChR2-XXL expression (no transgene expression was observed in effector controls; not shown). Animals were dissected in Ca^{2+}-free saline and brains were collected in 8 μL Ca^{2+}-free saline in a microtiter plate on ice. After all the brains had been collected (max. 3 brains per well), 4 μL Bouin's solution (HT10132, Sigma-Aldrich, Steinheim, Germany) were added for fixation. We note that transferring the brains directly to pure Bouin's solution would lead to a collapse of the tissue. The fixation time was 7 min, at room temperature on a shaker; initial experiments with fixation in 4% paraformaldehyde (PFA) had failed for the primary mouse anti-ChR2 antibody mentioned below (data not shown, see also Weiglein, Gerstner, Mancini, Schleyer, & Gerber, 2019, Schleyer et al., 2020). Then, the larval brains were washed three times consecutively in fresh washing solutions for 10 min each time, using 0.2% PBT (Triton-X-100, CAS: 9036-19-5, Roth, Karlsruhe, Germany; in 1x PBS). At each step, the larval brains were carefully transferred to another well. During washing, the well plate with the samples was stored on a shaker. The brains were incubated overnight with a primary monoclonal mouse anti-ChR2 antibody (clone 15E2, Cat No: 610180, RRID: N/A, ProGen Biotechnik, Heidelberg, Germany) diluted 1:100 in 0.2% PBT. A wet paper strip provided humidity, while well plates with the samples were covered in tinfoil and stored at 4 °C on a shaker. After three consecutive 10-min washing steps in 0.2% PBT on the next day, the larval brains were incubated with (i) a secondary polyclonal Cy3-conjugated goat anti-mouse antibody (Art-Nr. 115–165-071, RRID: AB_2338687, Jackson Immuno Research, Pennsylvania) and, (ii) as a reference signal for orienting in the preparation, with a polyclonal Alexa Fluor 488-conjugated goat anti-horseradish peroxidase (HRP) antibody (Art-Nr. 123–545-021, RRID: AB_2338965, Jackson Immuno Research, Pennsylvania), both diluted 1:300 in 0.2% PBT, for 1 hr at room temperature on a shaker. After three consecutive 10-min washing steps with 0.2% PBT, the samples were mounted in Vectashield (H-1000-10, Vector Laboratories Inc., Burlingame) on a cover slip.

In addition, we prepared whole mounts of larval brains from crosses from the respective driver strain and the 10xUAS-IVS-mCD8::GFP effector strain, as this allows a relatively better visualization of the respective DAN. Animals were dissected in Ca^{2+}-free saline and brains were collected in 15 μL Ca^{2+}-free saline in a microtiter plate on ice. Once the collection of brains was complete, they were transferred into 4% PFA (J19943, Alfa Aesar, Ward Hill; in PBS) and fixed for 30 min on a shaker. Afterwards, the brains were washed three times consecutively for 10 min each time and left overnight at 4 °C on a shaker incubated with the primary antibody mixture, consisting of (i) 4% normal goat serum (NGS; Art-Nr. 005–000-121, Jackson Immuno Research, Pennsylvania); (ii) a polyclonal rabbit anti-GFP antibody (A-11122, RRID: AB_221569, Invitrogen, Carlsbad), diluted 1:1000 in 0.2% PBT, and (iii) a monoclonal mouse anti-FAS II antibody (clone 1D4, anti-Fasciclin II DSHB, RRID: B_528235, Iowa), diluted 1:50 in 0.2% PBT. The next day, the brains were washed six times consecutively for 10 min each time and then incubated for 1 hr at room temperature on a shaker with the secondary antibody mixture, consisting of (a) a polyclonal Alexa 488-conjugated goat anti-rabbit antibody (A32731, RRID: AB_2633280, Thermo Fisher Scientific, Waltham), diluted 1:200 in 0.2% PBT, and (b) a polyclonal Cy3-conjugated goat anti-mouse antibody (details see above) diluted 1:200 in 0.2% PBT. After six consecutive 10-min washing steps, the brains were mounted in Vectashield on a cover slip.

Furthermore, to visualize predominantly pre−/postsynaptic regions of the respective DAN, we prepared whole mounts of larval brains from the driver strain crossed to the UAS-Dsyd-1::GFP/UAS-DenMark double effector strain. Animals were dissected as detailed above and brains were subsequently fixed for 20 min in 4% PFA. Afterwards, the brains were washed three times consecutively for

10 min each time and then transferred for 1.5 hr to a blocking solution consisting of 2% NGS. The brains were incubated for two nights at 4 °C on a shaker with the primary antibody mixture, consisting of i) 2% NGS, diluted 1:25 in 3% PBT; ii) a monoclonal rat anti-N-Cadherin antibody (DSHB, RRID:AB_10772277, Iowa), diluted 1:50 in 3% PBT (for background staining and better orientation in the preparation); iii) a polyclonal FITC-conjugated goat anti-GFP antibody (ab6662, RRID: AB_305635, Abcam, Cambridge, UK), diluted 1:1000 in 3% PBT (for visualization of the GFP-tag from UAS-Dsyd-1::GFP to label presynaptic regions), and iv) a polyclonal rabbit anti-DsRed antibody (632,496, RRID:AB_2571647, Clontech [TaKaRa Bio Inc], Kusatsu, Japan), diluted 1:200 in 3% PBT (for detecting the mCherry-tag from UAS-DenMark to label postsynaptic regions). After incubation, the brains were washed six times consecutively for 10 min each time and then incubated overnight at 4 °C with the secondary antibody mixture, consisting of i) 2% NGS, diluted 1:25 in 3% PBT; ii) a polyclonal Cy3-conjugated goat anti-rat antibody (A10522, RRID:AB_2534031, Life Technologies, Carlsbad), diluted 1:200 in 3% PBT, and iii) a polyclonal Cy5-conjugated goat anti-rabbit antibody (A10523, RRID: AB_2534032, Life Technologies, Carlsbad), diluted 1:200 in 3% PBT. After incubation, the brains were washed six times consecutively for 10 min each time and then mounted in Vectashield on a cover slip.

Image z-stacks were aquired with a Leica TCS SP8 confocal microscope (Leica Mikrosysteme Vertriebs GmbH, Wetzlar, Germany). Maximum intensity projections of z-stacks were done with Fiji software (RRID:SCR_002285). 3D-rendering and segmentation of predominantly pre- and postsynaptic regions were performed using Imaris software (Version 9.51, Bitplane, Zürich, Switzerland, RRID: SCR_007370, Oxford Instruments). Supplemental movies were produced in Imaris, too.

2.5 | Statistics

All behavioral data were analyzed using nonparametric statistics. One-sample sign tests (OSS; corresponding to binom.test, R Core Team, 2016) were applied for comparisons to chance levels (zero baseline). Kruskal–Wallis tests (KW) and Mann–Whitney U-tests (MWU) were used for between-group comparisons (Statistica 13, RRID:SCR_014213, StatSoft Inc, Tulsa). The *p*-value (*p*) of the KW test is indicated within the figures either as <.05 or > .05. In order to maintain an error rate below 5%, a Bonferroni–Holm (BH) correction for multiple comparisons was used throughout (Holm, 1979). Data are displayed as box plots with the median as the middle line, the box boundaries as 25% and 75% quantiles and the whiskers as 10% and 90% quantiles; the data are documented in the Supplementary Data file "Weiglein et al 2020 Raw Data".

3 | RESULTS

3.1 | DANs and drivers

At least two DANs have previously been reported to confer punishing effects: presenting an odor together with optogenetic activation of either DAN-f1 or DAN-d1, and possibly of DAN-g1, was found to establish odor avoidance in a subsequent test (Eschbach et al., 2020b). These neurons receive input from ascending pathways mediating aversive somatosensory cues and innervate the intermediate vertical lobe, the lateral appendix, and the lower vertical lobe compartments of the mushroom body, respectively (Eichler et al., 2017; Eschbach et al., 2020a; Saumweber et al., 2018) **(**Figure 1**)**. Within these compartments they host reciprocal synapses with the KCs, and connect to the compartments' cognate MBONs (Eschbach et al., 2020a, Saumweber et al., 2018). Outside the mushroom body they receive ascending input from *i.a*. touch and pain sensory pathways, as well as feedback originating from the MBONs (Eichler et al., 2017; Eschbach et al., 2020b; Eschbach et al., 2020a; Saumweber et al., 2018).

Before studying these neurons functionally, we assessed the expression from the driver strains as described in Saumweber et al. (2018) and Eschbach et al. (2020a). We confirmed strong and reliable expression from the respective drivers (Figures 3a,b,f,g and 4). Whereas for DAN-f1 and DAN-d1 these driver strains are also specific in expression, the driver covering DAN-g1 shows additional expression in the ventral nerve cord (Figure 4) (see also Eschbach et al., 2020a), prompting us to restrict further analyses to DAN-f1 and DAN-d1. As the following behavioral analyses of their function use third instar larvae throughout, we note that for both DAN-f1 and DAN-d1, the distribution of their predominantly pre- and postsynaptic regions as described from electron microscopy in a first instar larva (Eichler et al., 2017) was confirmed for third instar larvae at the light microscopic level: presynaptic regions are restricted to the above-mentioned compartments, and postsynaptic regions are more prominent outside the mushroom bodies, yet are present within the mushroom body compartments as well (Figure 3c-e,h-j; Movies 1-4).

3.2 | Temporal fingerprint and parametric features of the DAN-f1 teaching signal

To characterize the teaching signal from DAN-f1 we determined its temporal 'fingerprint'. That is, we expressed ChR2-XXL in DAN-f1 and optogenetically activated it with blue light at specific times relative to odor application. Specifically, the time from the onset of the 30-s light pulse to the beginning of the 30-s odor application is defined as the inter-stimulus-interval (ISI). As per convention, negative ISIs indicate that the odor is presented first and is followed by DAN-f1 activation in training (forward conditioning), whereas positive ISIs indicate by contrast that DAN-f1 activation comes first and is followed by the odor (backward conditioning). In both cases, reference groups are presented with the odor unpaired from DAN-f1 activation; the performance index (PI), as a measure of associative memory, reflects the difference in odor preference after training at the respective ISI versus the odor preference in the reference group. Positive PIs therefore reflect appetitive memory, whereas negative PIs reflect aversive memory. We note that this "timed" protocol differs in several respects from the "continuous" protocol used in Eschbach et al. (2020a). These include the duration and relative timing of odor presentation and DAN-activation (3 min

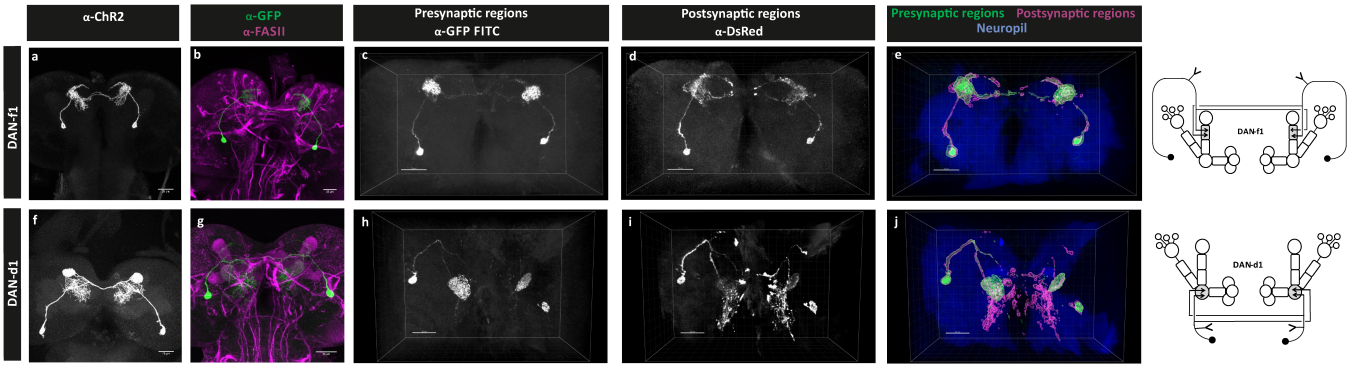

FIGURE 3 Transgene expression from the driver strains covering DAN-f1 and DAN-d1. (a) Whole-mount larval brains were prepared from the offspring of the driver strain covering DAN-f1 (SS02180) crossed to UAS-ChR2-XXL as the effector strain. Antibody staining with a primary mouse anti-ChR2 antibody and a secondary Cy3-conjugated goat anti-mouse antibody visualizes the expression pattern; a reference signal of an Alexa 488-conjugated anti-HRP antibody staining that we used for orienting in the preparation during image acquisition is not shown. (b) Whole mounts were prepared for the driver strain crossed to 10xUAS-IVS-mCD8::GFP, and expression patterns visualized by enhancing the GFP fluorescence signal with a primary rabbit anti-GFP antibody and a secondary Alexa 488-conjugated goat anti-rabbit antibody (green); to discern better the location of the respective DANs within the preparation a primary mouse anti-FAS II antibody and a secondary Cy3-conjugated goat anti-mouse antibody were used. (a, b) show maximum intensity projections. (c, d) Whole mounts were prepared for the driver strain crossed to UAS-Dsyd1::GFP/UAS-DenMark to visualize (c) predominantly presynaptic regions using a primary FITC-conjugated goat anti-GFP antibody (white) and (d) predominantly postsynaptic regions using a primary rabbit anti-DsRed antibody and a secondary Cy5-conjugated goat anti-rabbit antibody (white) for enhancing the fluorescence protein signal. **(e)** Predominantly pre- (green) and postsynaptic (magenta) regions were segmented and the corresponding surfaces generated in Imaris. To visualize the neuropil a primary rat anti-N-Cadherin antibody and a secondary Cy3-conjugated goat anti-rat antibody were used (blue). (c-e) show 3D-rendered representations. (f-j) Same as in (a-e), for the driver strain covering DAN-d1 (MB328b). Confocal z-stacks were acquired under a confocal microscope with a 63x glycerol objective (a-d, f-g) or a 40x oil objective (h-i). (e, j) are based on the z-stacks from (c, d) and (h, i), respectively. Scale bars indicate 25 μm. No transgene expression was observed outside the field of view. To the right of the panels, schematics of DAN-f1 and DAN-d1 are shown, respectively. A detailed characterization of these DANs by their lobe innervation, cell body location, lineage, major input regions, synaptic connectome, inputs activating them and (negative) results of immunochemistry for other transmitters can be found in Eichler et al. (2017), Saumweber et al. (2018) and Eschbach et al. (2020a)

each, nearly completely overlapping, in their case), the optogenetic effector and the wavelength of light used (Chrimson and red light in their case), as well as the addition of retinal to the food as a cofactor to boost the optogenetic effect of Chrimson. We further note that the handling as performed in Eschbach et al. (2020a) corresponds to a slightly negative ISI because odor is added to the Petri dish 1 min before the larvae are added onto it, and only then is the Petri dish with odor and larvae placed into the setup for optogenetic activation (C. Eschbach, Oxford, personal communication).

Our results show that the relative timing of odor application and DAN-f1 activation has a strong impact on memory scores, as indicated by a significant difference across groups **(**Figure 5a**)**. To see whether the aversive punishment memory after forward conditioning with an ISI of −10 s can be confirmed, we repeated the experiment including the appropriate genetic controls. Aversive memory was observed in the experimental genotype that expressed ChR2-XXL in DAN-f1, but not in the genetic controls heterozygous for only the ChR2-XXL effector, or only the DAN-f1 driver construct, respectively **(**Figure 5b**)**; indeed, memory scores in the experimental genotype differed from either of the genetic controls.

Relative to genetic controls, the trend for appetitive relief memory for backward conditioning at an ISI of 60 s was likewise verified **(**Figure 5a,c**)**. In fact, appetitive relief memory was further confirmed in a replication of the experiment, as well as both for slightly shorter and for slightly longer backward ISIs **(**Figure 6**)**. We note that it is expected in theory for aversive punishment memory to be stronger than appetitive relief memory (Solomon & Corbit, 1974; also see Figure 1a) and that for "real" electric shock punishments this is indeed the case (Gerber et al., 2019).

Furthermore, we found that aversive punishment memory decayed over time, remaining detectable until 10 min after training, whereas appetitive relief memory, starting out somewhat less strong already, was undetectable from 5 min on **(**Figure 7a,b**)**. This difference in the temporal stability of these memories qualitatively matches what has been reported for adult *Drosophila* (using odors and electric shock: Diegelmann et al., 2013). Interestingly, neither punishment memory nor relief memory increased by tripling the duration of DAN-f1 activation during training **(**Figure 7c,d**)**. This suggests that it is the timing of the onset and the offset, respectively, of DAN-f1 activation that is the major determinant for the teaching signal. We further observed that neither memory type was detectable after only one training trial with DAN-f1 activation **(**Figure 7e,f**)**, consistent with previous findings indicating that associative learning about taste punishments warrants multiple-trial training in the larva (Weiglein et al., 2019).

We next asked whether the teaching signal from activation of the DAN-d1 neuron, the second of the neurons under study, shares these features.

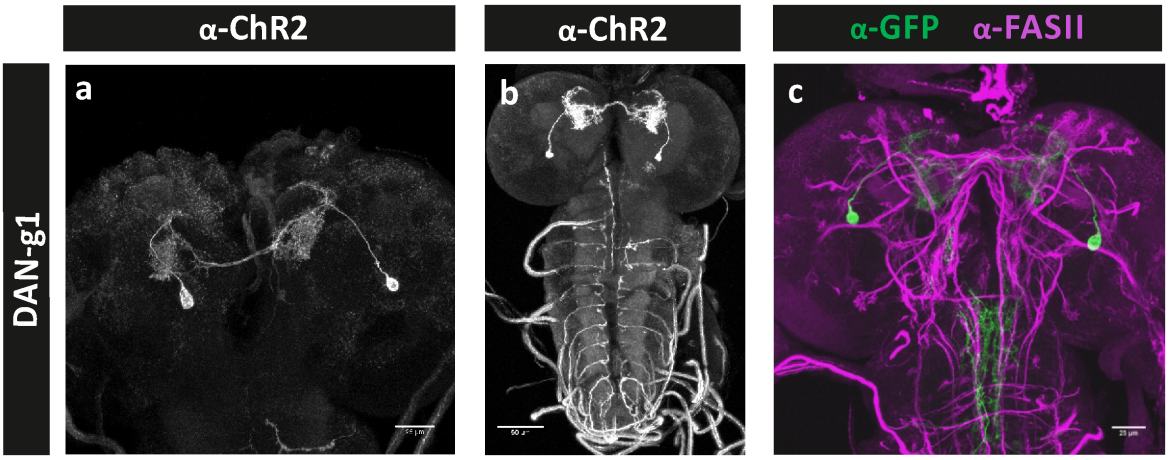

FIGURE 4 Transgene expression from the driver strain covering DAN-g1. (a) Whole-mount larval brains were prepared from the offspring of the driver strain covering DAN-g1 (SS01716) crossed to the effector strain UAS-ChR2-XXL. Antibody staining with a primary mouse anti-ChR2 antibody and a secondary Cy3-conjugated goat anti-mouse antibody visualizes the expression pattern of DAN-g1; a reference signal of an Alexa 488-conjugated anti-HRP antibody staining that we used for orienting in the preparation during image acquisition is not shown. (b) Preparation as in (a) showing both the brain hemispheres and the ventral nerve cord. Given the expression in the ventral nerve cord, this driver strain was not further investigated in behavioral experiments. (c) Whole mounts were prepared from the offspring of the same driver strain crossed to 10xUAS-IVS-mCD8::GFP. The fluorescence signal was enhanced by using a primary rabbit anti-GFP antibody and a secondary Alexa 488-conjugated goat anti-rabbit antibody (green); to discern better the location of the respective DANs in the preparation a primary mouse anti-FAS II antibody and a secondary Cy3-conjugated goat anti-mouse antibody were used. Confocal z-stacks were acquired under a confocal microscope with a 63x glycerol objective (a, c), or a 20x oil objective (b). Scale bars indicate 25 μm (a, c) or 50 μm (b)

3.3 | Temporal fingerprint and parametric features of the DAN-d1 teaching signal

For DAN-d1 too, the timing of its activation relative to odor application had an impact on memory scores, as indicated by a significant difference across groups (Figure 8a). In this case, however, our results suggest a single peak of aversive punishment memory at an ISI of about −10 s. Indeed, punishment memory for an ISI of −10 s was confirmed in a repetition of the experiment including genetic controls (Figure 8b). Although our initial results were not suggestive of any appetitive relief memory, we wondered whether relative to genetic controls, rather than relative to chance level (PI = 0), relief memory might be observed. However, for an ISI of 30 s, which appeared to be the relatively most promising candidate based on the ISI curve (Figure 8a), this was not the case (Figure 8c).

We further observed that the aversive punishment memory established through the DAN-d1 teaching signal was no longer detectable by 5 min after training (Figure 9a). A comparison across retention intervals did not reach significance, probably due to a floor effect. For the DAN-d1 teaching signal too, tripling the duration of activation did not increase the aversive punishment memory, suggesting that in the case of DAN-d1 it is also the onset of activation that is critical for an effective teaching signal (Figure 9b). Notably, an increase in the duration of activation did not reveal appetitive relief memory through DAN-d1, either (Figure 9c). Similar to what was shown in Figure 7 for DAN-f1 and for taste punishment in Weiglein et al. (2019), for DAN-d1 too one training trial was not sufficient to establish associative memory (Figure 9d).

3.4 | Specifically how do DAN-f1 and DAN-d1 memories affect behavior?

Given that forward conditioning with both DAN-f1 activation and DAN-d1 activation can establish punishment memories, we wondered whether these memories differ in how they specifically affect microbehavior. As recounted above, on a Petri dish surface *Drosophila* larvae typically move in a zig-zagging way, alternating between periods of relatively straight runs and lateral movements that we call head casts (HCs) (Gershow et al., 2012; Gomez-Marin et al., 2011; Gomez-Marin & Louis, 2014). After odor-taste punishment training, aversive memories have been shown i) not to affect run speed, but can be characterized by ii) a decrease in the number of HCs when moving away from the odor versus when moving towards the odor (i.e. a decrease in HC rate-modulation), and iii) a decreased propensity of HCs to align the larvae towards the odor (a decrease in the reorientation per HC) (Paisios, Rjosk, Pamir, & Schleyer 2017). From offline analyses of video recordings of the combined experiments shown in Figures 5-9 we observed the same to be the case for aversive punishment memories established by forward conditioning with either DAN-f1 activation (Figure 10ai,bi,ci) or DAN-d1 activation (Figure 10aii,bii,cii). Of note is that appetitive memories are usually

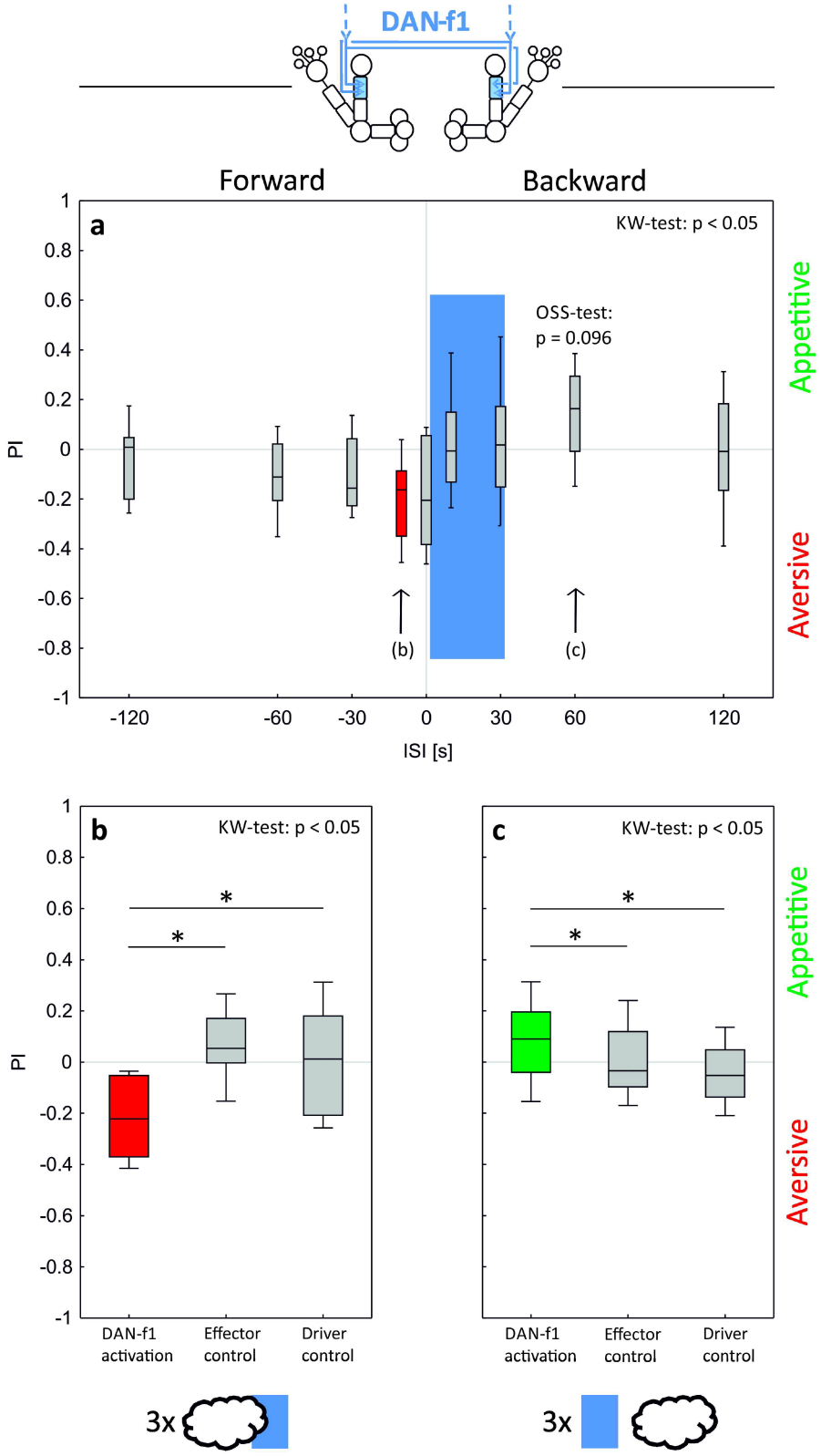

FIGURE 5 Temporal fingerprint of the DAN-f1 teaching signal. Larval offspring of the driver strain covering DAN-f1 crossed to UAS-ChR2-XXL as the effector strain underwent three training trials pairing the odor *n*-amylacetate with optogenetic activation of DAN-f1 by blue light, at the indicated inter-stimulus-interval (ISI). Negative ISIs mean that the odor preceded the light activation (forward), whereas positive values mean that light activation preceded the odor (backward). In all cases, reference groups of larvae received DAN-f1 activation unpaired from the odor. The performance index (PI), as a measure for associative memory, reflects the difference in odor preference after paired versus unpaired training. Positive PIs reflect appetitive memory, whereas negative PIs reflect aversive memory. (a) The relative timing of the odor and the DAN-f1 activation had a significant impact on memory performance ($p < .05$ in a Kruskal–Wallis test). Forward conditioning resulted in aversive punishment memory (ISI = −10 s), whereas in this dataset only a tendency for appetitive relief memory upon backward conditioning (ISI = 60 s) was observed. (b) Validation of aversive punishment memory upon forward conditioning at an ISI of −10 s, in comparison to genetic controls heterozygous for only the effector, or only the driver, respectively. (c) Appetitive relief memory upon backward conditioning at an ISI of 60 s, relative to genetic controls heterozygous for only the effector, or only the driver, respectively. Sample sizes are for (a) N = 19; 19; 19; 19; 19; 18; 18; 19; 19, (b) all N = 12, (c) all N = 53. Data are displayed as box plots, with the median indicated by the middle line, the box boundaries indicating 25 and 75% quantiles, and the whiskers 10 and 90% quantiles. Red fill indicates aversive punishment memory relative to chance levels (PI = 0) with Bonferroni-Holm-corrected one-sample sign tests (OSS-tests) ($p < .05$); green fill correspondingly indicates appetitive relief memory. Both in (b) and in (c) Kruskal-Wallis tests (KW-tests) reveal significance across groups ($p < .05$); * refers to Bonferroni-Holm-corrected pairwise comparisons with Mann–Whitney U-tests ($p < .05$). The training procedure is indicated in sketches to the bottom of (b) and (c): blue bars indicate blue light for optogenetic activation of DAN-f1; white clouds indicate the odor *n*-amylacetate. The preference values underlying the PIs are documented and visualized in the "Weiglein et al 2020 Raw Data" file [Color figure can be viewed at wileyonlinelibrary.com]

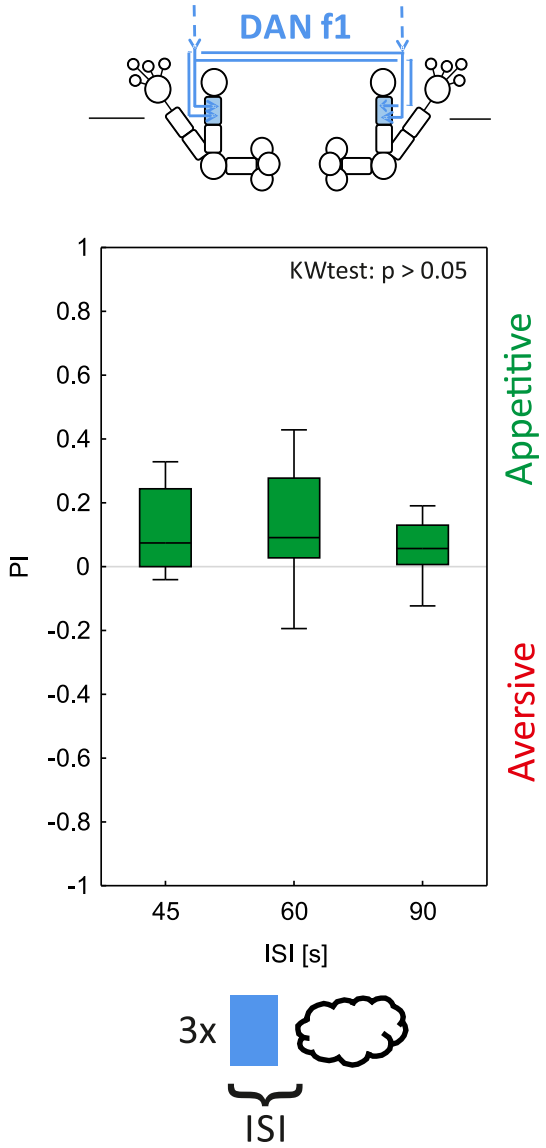

FIGURE 6 Confirmation of relief memory through backward conditioning with DAN-f1. Larval offspring of the driver strain covering DAN-f1 crossed to UAS-ChR2-XXL as the effector strain underwent three training trials comprising backward conditioning of the odor n-amylacetate with optogenetic activation of DAN-f1 by blue light, at the indicated inter-stimulus-interval (ISI) of either 45, 60 or 90 s. In all cases, reference groups of larvae received light activation unpaired from the odor. The performance index (PI), as a measure of associative memory, reflects the difference in odor preference after paired versus unpaired training. Positive memory scores reflect appetitive memory. Sample sizes are for all N = 19. A Kruskal–Wallis test across groups was not significant ($p > .05$). Green fill indicates appetitive relief memory relative to chance levels (PI = 0) with Bonferroni–Holm-corrected one-sample sign tests ($p < .05$). The training procedure is indicated in the sketch at the bottom: the blue rectangle indicates blue light for optogenetic activation of DAN-f1; white clouds indicate the odor n-amylacetate. The preference values underlying the PIs are documented and visualized in the "Weiglein et al 2020 Raw Data" file [Color figure can be viewed at wileyonlinelibrary.com]

characterized by the opposite modulations of HC rate and direction (Paisios, Rjosk, Pamir, & Schleyer 2017; Schleyer et al., 2015; Thane, Viswanathan, Meyer, Paisios & Schleyer 2019). Regarding the (relatively weak) relief memory established through backward conditioning with DAN-f1, we detected an increased propensity to align towards the odor, but no modulation of HC rate (Figure 10aiii,biii,ciii).

4 | DISCUSSION

4.1 | Heterogeneity in the temporal fingerprints of teaching signals in *Drosophila* and its implications

The present study reveals qualitative differences in the temporal fingerprint of teaching signals from two larval DANs in the aversive domain (Figure 11). Optogenetic activation of DAN-f1 can mediate both punishment memory upon forward conditioning with an odor and relief memory upon backward conditioning, and can thus establish timing-dependent valence reversal. In contrast, for DAN-d1 only punishment memory upon forward conditioning is observed, with a relatively narrow window of effective intervals compared to DAN-f1. Similar heterogeneity of teaching signals in the aversive domain has been reported in adult *Drosophila*, with timing-dependent valence reversal observed for PPL1-01 but not—or not robustly—for the other tested cases (Aso & Rubin, 2016; König et al., 2018). Thus, in the aversive domain teaching signals from different DANs allow for more or less broadly defined coincidences with environmental cues to be established, with some DANs actually reflecting the relative temporal structure within the aversive event.

In the case of the larva a neuron that "mirrors" the teaching signal of DAN-f1 in the appetitive domain has been found (Saumweber et al., 2018, loc. Cit. Figure 6). Forward conditioning of an odor with DAN-i1 activation establishes learned odor approach (reward memory), whereas backward conditioning establishes odor avoidance ("frustration" memory). Whether this temporal fingerprint is shared by DAN-h1, the other DAN that can be of rewarding effect (Saumweber et al., 2018), is not known. In adults and regarding the appetitive domain, Aso and Rubin (2016) found relatively broad windows of coincidence for two sets of DANs from the PAM cluster (defined by the drivers MB213B and MB315C/MB109B), yet no timing-dependent valence reversal in either case. More recently, Handler et al. (2019) used a behavioral paradigm that allows training with more precise stimulus timing and revealed timing-dependent valence reversal in the appetitive domain for a relatively broad set of DANs from the PAM cluster (defined by the R58E02 driver).

In any event, in the case of the larva the present study together with Saumweber et al. (2018) suggests an elegantly simple architecture of the single, identified DAN-f1 and DAN-i1 neurons mediating oppositely valenced teaching signals for the occurrence and the termination of aversive and appetitive events, respectively. This is consistent with both the scenario put forward by Handler et al. (2019) for

adults, more broadly referring to DANs of the PPL cluster versus those of the PAM cluster (defined by the drivers R58E02 and 52H03, respectively), and with classical theoretical proposals of reinforcement learning (Malaka, 1999). Indeed, such an organization of an association system should be versatile enough to decipher the causal structure within events of motivational significance (Dickinson, 2001). In contrast, DANs establishing "mere coincidence"—such as DAN-d1 with its notably narrower effective time window—may rather allow two coincident inputs to be bound together into one mnemonic object. In what he called "an experiment into synthetic psychology", such a separation into event- and object-learning has been proposed by Braitenberg (1984).

4.2 | Molecular mechanisms of timing-dependent valence reversal

The molecular mechanisms underlying timing-dependent valence reversal are beginning to be uncovered in adult *Drosophila*. In an explant brain preparation and with respect to the appetitive domain, Handler et al. (2019) found that forward pairing of Kenyon cell activity and activation of the above-mentioned, relatively broad set of PAM neurons leads to a depression of the KC-to-MBON synapse in the γ4 compartment, whereas backward pairings lead to potentiation. These effects are abolished in Dop1R1 and Dop1R2 receptor mutants, respectively. Strikingly, the optima for coincidence detection in these two molecular pathways are slightly offset, such that cAMP signals mediated via the Dop1R1/ Gαs/ AC pathway peak for

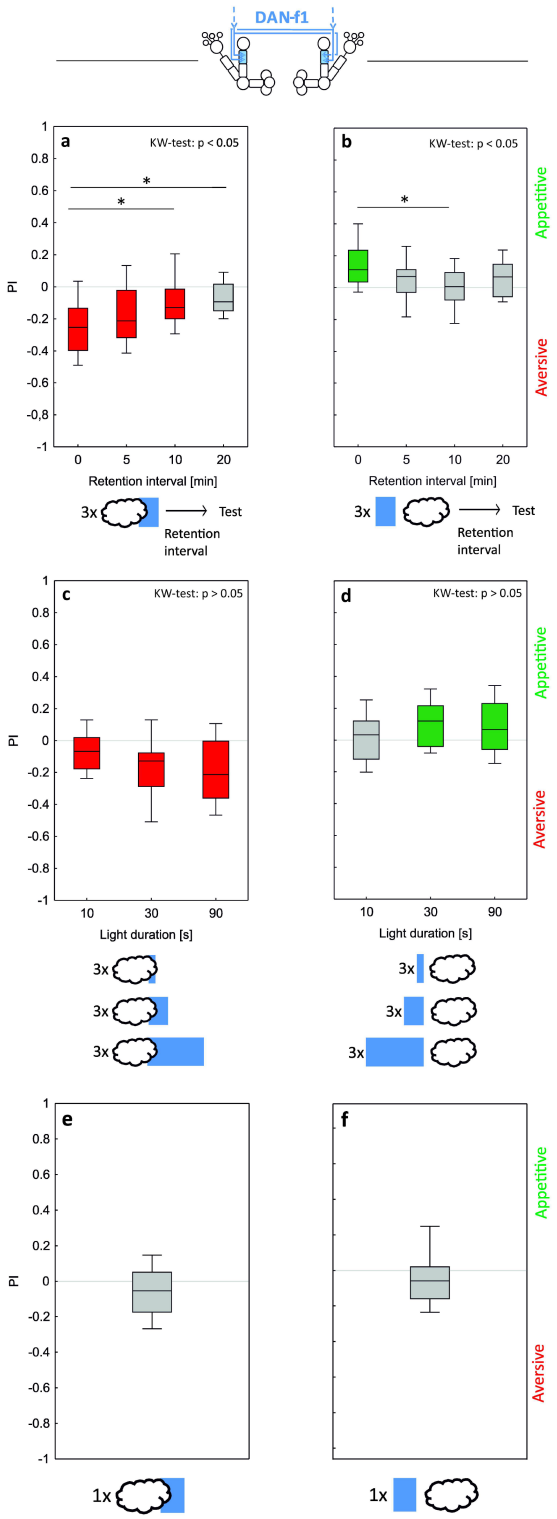

FIGURE 7 Parametric features of the DAN-f1 teaching signal. Larval offspring of the driver strain covering DAN-f1 crossed to UAS-ChR2-XXL as the effector strain underwent training with the odor *n*-amylacetate and optogenetic activation of DAN-f1 by blue light as in Figure 5. (a) Animals were either tested for their odor preference immediately after training (retention interval 0), or were collected and left to wait in a water droplet for 5, 10, or 20 min until that test was performed. Forward conditioning at an ISI of −10 s leads to aversive punishment memory that is detectable until at least 10 min after training. (b) For the same retention intervals as in (a), backward conditioning at an ISI of 60 s leads to appetitive relief memory that is detectable only immediately after training. (c) The duration of DAN-activation during training was either 10, 30, or 90 s; this corresponds to activations of either a third of the duration, of the same duration, or of a duration prolonged threefold relative to those used in Figure 5. For forward ISIs of −10 s, i.e. for cases in which the timing of the onset of DAN-f1 activation relative to odor was maintained but the duration of this activation was varied, animals showed aversive punishment memory for all activation durations tested. (d) For a backward ISI of 60 s, i.e. for cases with a constant timing between the offset of DAN-f1 activation and odor, comparably strong appetitive relief memory was detectable across activation durations. (e) After only one training trial at a forward ISI of −10 s, no aversive punishment memory was detectable. (f) Similarly, after only one training trial at a backward ISI of 60 s, no appetitive relief memory was observed. Sample sizes are for (a) all $N = 20$, (b) all $N = 28$, (c) all $N = 24$, (d) $N = 42; 42; 43$, (e) all $N = 20$, (f) all N = 20. Red fill indicates aversive punishment memory relative to chance levels (PI = 0) with Bonferroni-Holm-corrected one-sample sign tests ($p < .05$); green fill correspondingly indicates appetitive relief memory. Both in (a) and in (b) Kruskal–Wallis tests reveal significance across groups ($p < .05$), whereas this was not the case for (c) and (d); * refers to Bonferroni–Holm-corrected pairwise comparisons with Mann–Whitney U-tests ($p < .05$). The preference values underlying the PIs are documented and visualized in the "Weiglein et al 2020 Raw Data" file. Other details as in the legend of Figure 5 [Color figure can be viewed at wileyonlinelibrary.com]

coincidence, whereas the Ca^{2+} signals mediated via the Dop1R2/Gαq/ IP3 pathway peak for short backward intervals. At the behavioral level, using a high-temporal-resolution assay, neither mutant can follow repeated reversals of forward and backward conditioning; notably, the net effect of such repeated reversals in Dop1R1 mutants corresponds to backward conditioning (frustration memory), whereas in Dop1R2 mutants it corresponds to forward conditioning (reward memory). These findings suggest that the concerted action of the Dop1R1 and Dop1R2 pathways underlies timing-dependent valence reversal.

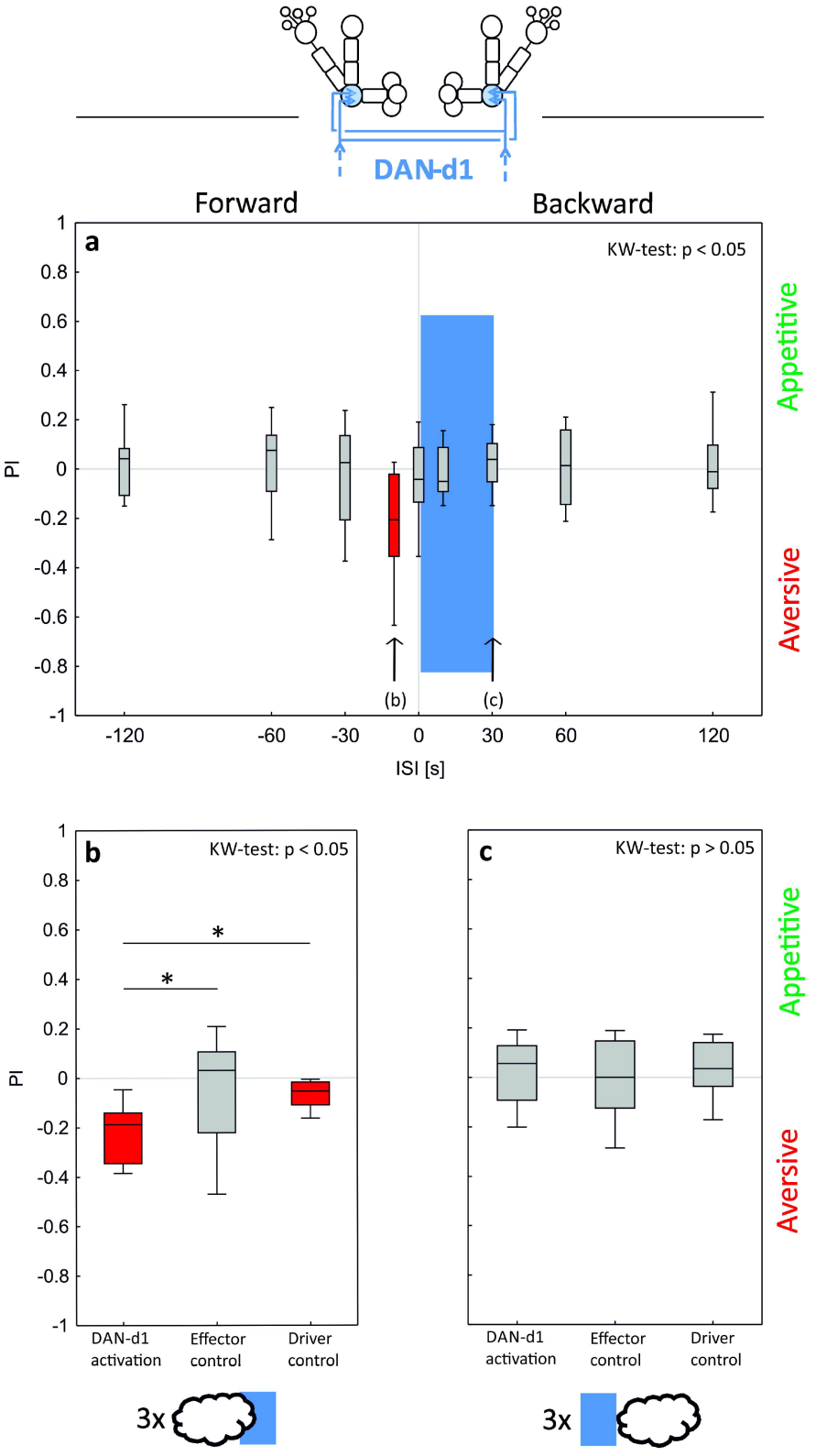

FIGURE 8 Temporal fingerprint of the DAN-d1 teaching signal. Larval offspring of the driver strain covering DAN-d1 crossed to UAS-ChR2-XXL as the effector strain underwent training with the odor *n*-amylacetate and optogenetic activation of DAN-d1 by blue light as in Figure 5. (a) The relative timing of the odor and the DAN-d1 activation had a significant impact on memory performance ($p < .05$ in a Kruskal–Wallis test). Forward conditioning resulted in aversive punishment memory (ISI = −10 s). (b) Validation of aversive punishment memory upon forward conditioning at an ISI of −10 s, in comparison to genetic controls heterozygous for only the effector, or only the driver, respectively. (c) Also relative to genetic controls, no appetitive relief memory was observed upon backward conditioning at an ISI of 30 s, confirming the lack of any trend for such relief memory relative to chance level (PI = 0) in (a). Sample sizes are for (a) all $N = 19$, (b) all $N = 16$, (c) all $N = 20$. Red fill indicates aversive punishment memory relative to chance levels (PI = 0) with Bonferroni-Holm-corrected one-sample sign tests ($p < .05$). In (b) a Kruskal-Wallis test reveals significance across groups ($p < .05$) whereas such a comparison was not significant in (c) ($p > .05$); * refers to Bonferroni-Holm-corrected pairwise comparisons with Mann–Whitney U-tests ($p < .05$). The training procedure is indicated in sketches to the bottom of (b) and (c): blue bars indicate blue light for optogenetic activation of DAN-f1; white clouds indicate the odor *n*-amylacetate. The preference values underlying the PIs are documented and visualized in the "Weiglein et al 2020 Raw Data" file. Other details as in Figure 5 [Color figure can be viewed at wileyonlinelibrary.com]

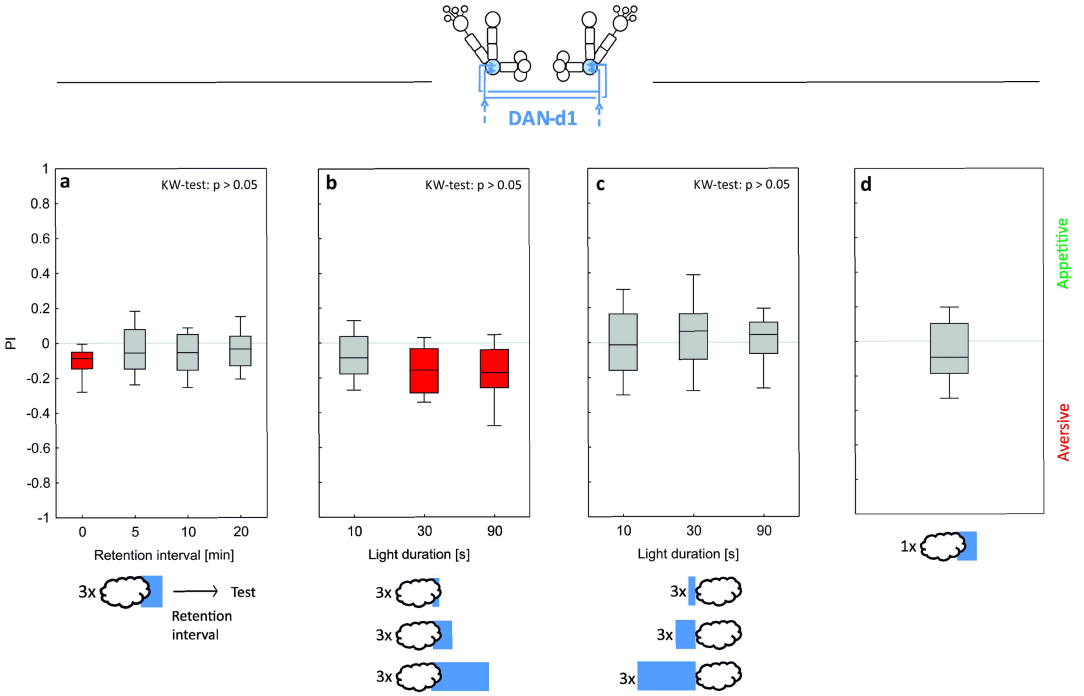

FIGURE 9 Parametric features of the DAN-d1 teaching signal. Larval offspring of the driver strain covering DAN-d1 crossed to UAS-ChR2-XXL as the effector strain underwent training with the odor *n*-amylacetate and optogenetic activation of DAN-d1 by blue light as in Figure 5. (a) As in Figure 7a animals were either tested directly after the training (retention interval 0), or they were collected after the training, left to wait in a water droplet for either 5, 10, or 20 min, and only then tested for their preference. Forward conditioning at an ISI of −10 s led to punishment memory when animals were tested immediately after training, whereas no such aversive memory was observable for any other retention interval. (b) As in Figure 7c, the duration of activation during training was either 10, 30, or 90 s, and thus either a third of the duration, the same duration, or a duration prolonged threefold relative to those used in Figures 5 and 8. For forward ISIs of −10 s, i.e. for cases in which the timing of the onset of DAN-d1 activation relative to odor was maintained but the duration of activation was varied, there was no significant effect across activation durations. Testing each case against chance levels (PI = 0) suggests that animals showed aversive punishment memory for activation durations of 30 and 90 s but not for shorter durations. (c) For the backward ISI of +30 s, i.e. cases with a constant timing between the offset of DAN-d1 activation and odor, no appetitive relief memory was detectable, irrespective of activation duration. (d) As in Figure 7e, no aversive punishment memory was detectable after one forward conditioning training trial at an ISI of −10 s. Sample sizes are for (a) N = 26; 24; 24; 23, (b) all N = 35, (c) all N = 16, (d) N = 28. Red fill indicates aversive punishment memory relative to chance levels (PI = 0) with Bonferroni-Holm-corrected one-sample sign tests ($p < .05$). Neither in (a), (b), or (c) did Kruskal-Wallis tests reveal significance across groups ($p < .05$). The preference values underlying the PIs are documented and visualized in the "Weiglein et al 2020 Raw Data" file. Other details as in the legend of Figure 5 [Color figure can be viewed at wileyonlinelibrary.com]

Regarding the association of odor and electric shock, both forward and backward conditioning are impaired upon of a lack of synapsin (Niewalda et al., 2015). Synapsin is an evolutionarily conserved presynaptic protein with a high number of phosphorylation sites, and consensus motifs for multiple kinases (reviewed in Diegelmann et al., 2013; see also Niewalda et al., 2015, Kleber et al., 2016, Blanco-Redondo et al., 2019). Synapsin regulates the balance between reserve and readily-releasable synaptic vesicle pools, and hence synaptic efficacy, across species (Benfenati, 2011; Diegelmann et al., 2013; Hilfiker et al., 1999). This raises the possibility that molecular cascades originating from the Dop1R1 and Dop1R2 pathways are integrated on synapsin as a common effector.

Interestingly, in parallel to the "canonical" punishment memory component established via dopamine signaling from the PPL1-01 neuron during forward conditioning, nitric oxide signaling from this neuron supports an appetitively valenced memory component (Aso et al., 2019). Such nitric oxide signaling seems to be dispensable for relief memory after backward conditioning (Aso et al., 2019; loc. Cit. Figure 5-S3). This would be consistent with the above scenario of timing-dependent valence reversal via the concerted action of the Dop1R1 and Dop1R2 pathways. However, König et al. (2018) found that an RNAi knock-down of the tyrosine hydroxylase (TH) enzyme in PPL1-01 impairs punishment memory through forward conditioning with this neuron, but not relief memory established by backward conditioning. This raises the possibility of a nondopaminergic mechanism for relief memory formation, or at least a mechanism not affected by TH-RNAi in the PPL1-01 neuron. We note that in order to account for the heterogeneity of teaching signals from DANs, the scenario of Dop1R1/R2 function conferring timing-dependent valence reversal would suggest a correspondingly heterogeneous expression of these two receptors across compartments, which to the best of our knowledge has not been observed.

In summary and with the above-mentioned caveats in mind, the best working hypothesis still seems to be that timing-dependent

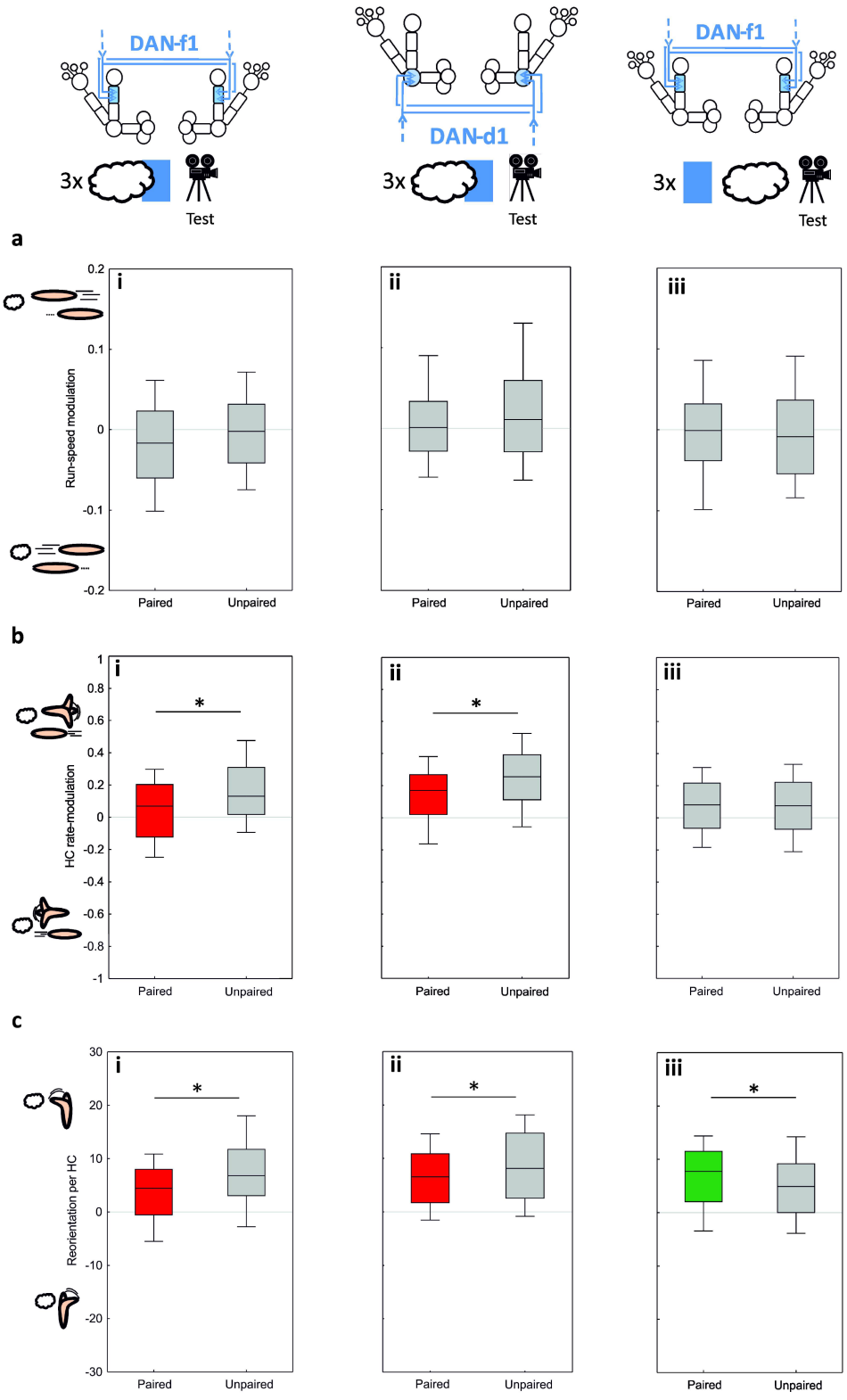

FIGURE 10 Specifically how do DAN-f1 and DAN-d1 memories affect behavior? Larvae were video-tracked for offline analyses of the modulations of locomotion after paired or unpaired training with odor and DAN activation. (a) No significant difference in run speed-modulation was observed between paired and unpaired trained animals for (i) DAN-f1 forward and (ii) DAN-d1 forward conditioning, nor for (iii) DAN-f1 backward conditioning. However, paired-trained and unpaired-trained animals differed significantly regarding (b) the modulation of head cast (HC) rate in the case of both (i) DAN-f1 forward and (ii) DAN-d1 forward conditioning, such that after paired training larvae make fewer HCs while heading away from the odor source, and more HCs while heading towards it. (iii) For DAN-f1 backward conditioning no significant difference in the modulation of HC rate was observed. (c) In addition, paired-trained and unpaired-trained animals for both (i) DAN-f1 forward and (ii) DAN-d1 forward conditioning showed a significant difference in the HC direction relative to the odor, such that after paired training larvae direct their HCs more away from the odor source than after unpaired training. (iii) For backward conditioning with DAN-f1, the opposite was observed. Corresponding PI scores for (i) can be found in Figures 5 and 7; for (ii) in Figures 8 and 9; and for (iii) in Figures 5–7; in some instances, video-tracking data were unavailable for technical reasons. Sketches of larvae depict their change in behavior with respect to the odor in the case of positive or negative scores. Sample sizes are for (ai, bi, ci) $N = 76; 74$, for (aii, bii, cii) $N = 134; 122$, (aiii, biii, ciii) $N = 143; 147$. Colored fill indicates significant Bonferroni-Holm-corrected Mann–Whitney U-tests ($p < .05$) for cases reflecting aversive punishment memory (red) and appetitive relief memory (green). The paired training procedure is indicated in sketches to the top of the figures: blue bars indicate blue light for optogenetic activation of the respective DAN; white clouds indicate the odor *n*-amylacetate [Color figure can be viewed at wileyonlinelibrary.com]

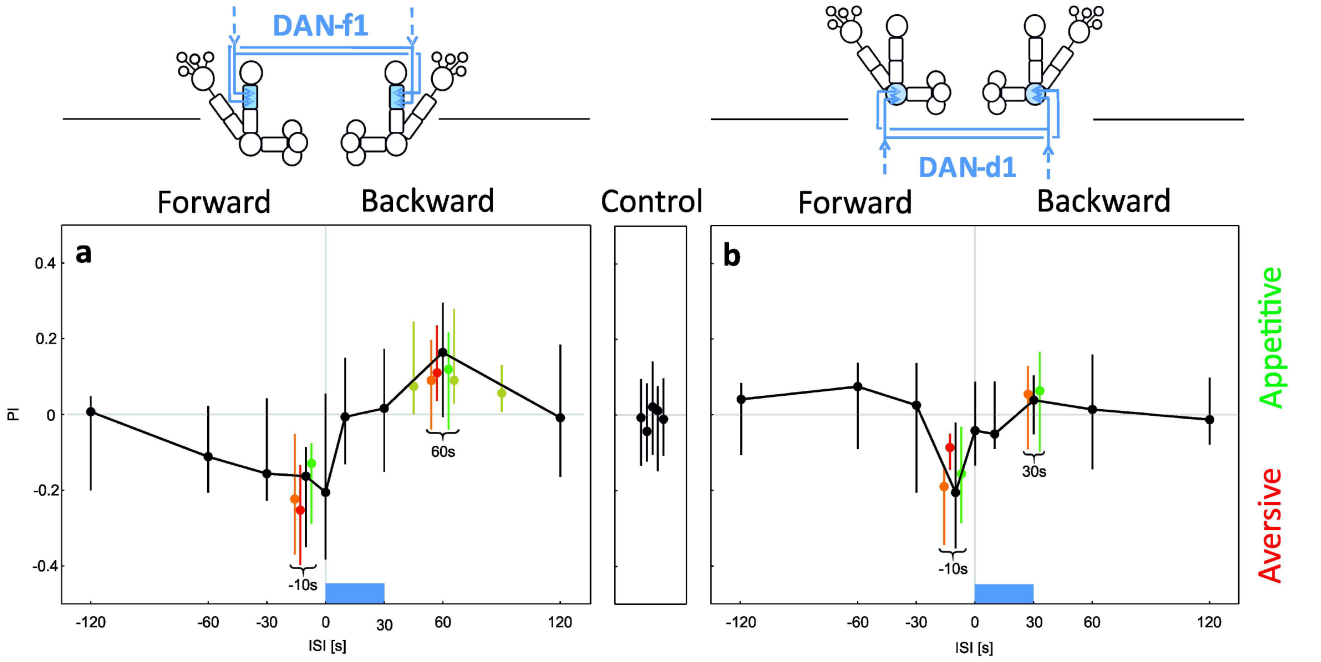

FIGURE 11 Summary of the temporal fingerprints of the teaching signals from DAN-f1 and DAN-d1. (a) For optogenetic activation of DAN-f1 (sketched at the top) the median PI scores together with the 25 and 75% quantiles are plotted against the timing of this activation in relation to odor presentation (the inter-stimulus-interval, ISI) (black Figure 5a; orange Figure 5b,c; red Figure 7a,b; green Figure 7c,d; beige Figure 6, in all cases of the experimental genotype and the standard training procedure). In the middle panel, respectively pooled medians of the PI scores from the genetic controls for DAN-f1 (Figure 5b,c) and DAN-d1 (Figure 8b,c) as well as from the longest ISI of each experimental genotype (Figure 5a, Figure 8a) are plotted as Control. (b) As in (a), for DAN-d1 (black Figure 8a; orange Figure 8b,c; red Figure 9a; green Figure 9b, c). The data underlying these median PIs are documented and visualized in the "Weiglein et al 2020 Raw Data" file. For ISIs where multiple datasets are available, the medians and quantiles are plotted slightly offset, as indicated by the curly brackets [Color figure can be viewed at wileyonlinelibrary.com]

valence reversal by the activation of DANs in adult *Drosophila* comes about through the differential recruitment of Dop1R1 and Dop1R2 signaling. Whether this holds true for the larva too, whether it applies for "real world" reinforcers such as sugar or electric shock, whether such a scenario can explain the heterogeneity in the temporal fingerprint of teaching signals from dopaminergic neurons, and whether this reflects a cross-species principle, remains to be determined.

ACKNOWLEDGMENTS

Discussions with Christian König (LIN), Markus Fendt (OVGU Magdeburg), Robert Kittel (U Leipzig) and technical assistance by Frank Unterstab and Marko Dombach (LIN) are gratefully acknowledged. We thank Oliver Kobler (LIN) for an introduction to Imaris and comments on earlier versions of the manuscript, Naoko Toshima (LIN) for allowing us to use her larval sketches in Figure 10, and R.D.V. Glasgow (Zaragoza, Spain) for language editing. Open Access funding enabled and organized by ProjektDEAL.

CONFLICT OF INTEREST

The authors declare no competing interests.

AUTHOR CONTRIBUTIONS

AW, MS and BG designed the experiments, AW, JT, IF, LW and NM performed the experiments, AW did the statistical analyses on the data, AW and BG wrote the manuscript with input from all authors.

DATA AVAILABILITY STATEMENT

The data are documented in the Supplementary Data file 'Weiglein et al 2020 Raw Data'.

ORCID

Alićе Weiglein https://orcid.org/0000-0003-4626-328X
Bertram Gerber https://orcid.org/0000-0003-3003-0051

REFERENCES

Almeida-Carvalho, M. J., Berh, D., Braun, A., Chen, Y. C., Eichler, K., Eschbach, C., … Zlatic, M. (2017). The Ol1mpiad: Concordance of behavioural faculties of stage 1 and stage 3 *Drosophila* larvae. *The Journal of Experimental Biology*, *220*, 2452–2475. https://doi.org/10.1242/jeb.156646

Appel, M., Scholz, C. J., Kocabey, S., Savage, S., König, C., & Yarali, A. (2016). Independent natural genetic variation of punishment- versus relief-memory. *Biology Letters*, *12*, 20160657. https://doi.org/10.1098/rsbl.2016.0657

Aso, Y., & Rubin, G. (2016). Dopaminergic neurons write and update memories with cell-type-specific rules. *eLife*, *5*, e16135. https://doi.org/10.7554/eLife.16135

Aso, Y., Ray, R. P., Long, X., Bushey, D., Cichewicz, K., Ngo, T. T., … Rubin, G. M. (2019). Nitric oxide acts as a cotransmitter in a subset of dopaminergic neurons to diversify memory dynamics. *eLife*, *8*, e49257. https://doi.org/10.7554/eLife.49257

Aso, Y., & Rubin, G. M. (2020). Toward nanoscale localization of memory engrams in *Drosophila*. *Journal of Neurogenetics*, *34*, 151–155. https://doi.org/10.1080/01677063.2020.1715973

Benfenati, F. (2011). Synapsins – Molecular function, development and disease. *Seminars in Cell & Developmental Biology*, *22*, 377–434. https://doi.org/10.1016/j.semcdb.2011.07.007

Blanco-Redondo, B., Nuwal, N., Kneitz, S., Nuwal, T., Halder, P., Liu, Y., … Buchner, E. (2019). Implications of the Sap47 null mutation for synapsin phosphorylation, longevity, climbing proficiency and behavioural plasticity in adult *Drosophila*. *J Exp Biol*, *222*, jeb203505. https://doi.org/10.1242/jeb.203505

Boto, T., Stahl, A., & Tomchik, S. M. (2020). Cellular and circuit mechanisms of olfactory associative learning in *Drosophila*. *Journal of Neurogenetics*, *34*, 36–46. https://doi.org/10.1080/01677063.2020.1715971

Braitenberg, V. (1984). *Vehicles: Experiments in synthetic psychology*. Cambridge, Massachusetts: MIT Press.

Cognigni, P., Felsenberg, J., & Waddell, S. (2018). Do the right thing: Neural network mechanisms of memory formation, expression and update in *Drosophila*. *Current Opinion in Neurobiology*, *49*, 51–58. https://doi.org/10.1016/j.conb.2017.12.002

Dawydow, A., Gueta, R., Ljaschenk, D., Ullrich, S., Hermann, M., Ehmann, N., … Kittel, R. J. (2014). Channelrhodopsin-2-XXL, a powerful optogenetic tool for low-light applications. *Proc Natl Acad Sci USA*, *111*, 13972–13977. https://doi.org/10.1073/pnas.1408269111

Dickinson, A. (2001). The 28th Bartlett memorial lecture. Causal learning: An associative analysis. *The Quarterly Journal of Experimental Psychology. B*, *54*, 3–25. https://doi.org/10.1080/02724990042000010

Diegelmann, S., Preuschoff, S., Appel, M., Niewalda, T., Gerber, B., & Yarali, A. (2013). Memory decay and susceptibility to amnesia dissociate punishment- from relief-learning. *Biology Letters*, *9*, 20121171. https://doi.org/10.1098/rsbl.2012.1171

Eichler, K., Li, F., Litwin-Kumar, A., Park, Y., Andrade, I., Schneider-Mizell, C. M., … Cardona, A. (2017). The complete connectome of a learning and memory Centre in an insect brain. *Nature*, *548*, 175–183. https://doi.org/10.1038/nature23455

Eschbach, C., Fushiki, A., Windig, M., Schneider-Mizell, C. M., Shao, M., Arruda, R., … Zlatic, M. (2020a). Recurrent architecture for adaptive regulation of learning in the insect brain. *Nature Neuroscience*, *23*, 544–555. https://doi.org/10.1038/s41593-020-0607-9

Eschbach C., Fushiki A., Windig M., Afonso B., Andrade I.V., Cocanougher B. T., Eichler K., Gepner R., Si G., Valdes-Aleman J., Gershow M., Jefferis G. S.X.E., Truman J.W., Fetter R.D., Samuel A., Cardona A., Zlatic M. (2020b). Circuits for integrating learnt and innate valence in the fly brain. *bioRxiv*: https://doi.org/10.1101/2020.04.23.058339.

Gerber, B., & Hendel, T. (2006). Outcome expectations drive learned behaviour in larval *Drosophila*. *Proceedings of the Biological Sciences*, *273*, 2965–2968. https://doi.org/10.1098/rspb.2006.3673

Gerber, B., & Stocker, T. (2007). The *Drosophila* larva as a model for studying chemosensation and chemosensory learning: A review. *Chemical Senses*, *32*, 65–89. https://doi.org/10.1093/chemse/bjl030

Gerber, B., Yarali, A., Diegelmann, S., Wotjak, C. T., Pauli, P., & Fendt, M. (2014). Pain-relief learning in flies, rats and man: Basic research and applied perspectives. *Learning & Memory*, *21*, 232–252. https://doi.org/10.1101/lm.032995.113

Gerber, B., König, C., Fendt, M., Andreatta, M., Romanos, M., Pauli, P., & Yarali, A. (2019). Timing-dependent valence reversal: A principle of reinforcement processing and its possible implications. *Current Opinion in Behavioral Sciences*, *26*, 114–120. https://doi.org/10.1016/j.cobeha.2018.12.001

Gerhard, S., Andrade, I., Fetter, R. D., Cardona, A., & Schneider-Mizell, C. M. (2017). Conserved neural circuit structure across *Drosophila* larval development revealed by comparative connectomics. *eLife*, *6*, e29089. https://doi.org/10.7554/eLife.29089

Gershow, M., Berck, M., Mathew, D., Luo, L., Kane, E. A., Carlson, J. R., & Samuel, A. D. (2012). Controlling airborne cues to study small animal navigation. *Nature Methods*, *9*, 290–296. https://doi.org/10.1038/nmeth.1853

Gomez-Marin, A., Stephens, G. J., & Louis, M. (2011). Active sampling and decision making in *Drosophila* chemotaxis. *Nat Com*, *2*, 441. https://doi.org/10.1038/ncomms1455

Gomez-Marin, A., & Louis, M. (2014). Multilevel control of run orientation in *Drosophila* larval chemotaxis. *Frontiers in Behavioral Neuroscience*, *8*, 38. https://doi.org/10.3389/fnbeh.2014.00038

Handler, A., Graham, T. G. W., Cohn, R., Morantte, I., Siliciano, A. F., Zeng, J., … Ruta, V. (2019). Distinct dopamine receptor pathways underlie the temporal sensitivity of associative learning. *Cell*, *178*, 60–75. https://doi.org/10.1016/j.cell.2019.05.040

Heisenberg, M. (2003). Mushroom body memoir: From maps to models. *Nature Reviews. Neuroscience*, *4*, 266–275. https://doi.org/10.1038/nrn1074

Hellstern, F., Malaka, R., & Hammer, M. (1998). Backward inhibitory learning in honeybees: A behavioral analysis of reinforcement processing. *Learning & Memory*, *4*, 429–444. https://doi.org/10.1101/lm.4.5.429

Hilfiker, S., Pieribone, V. A., Czernik, A. J., Kao, H. T., Augustine, G. J., & Greengard, P. (1999). Synapsins as regulators of neurotransmitter release. *Philosophical Transactions of the Royal Society of London. Series B, Biological Sciences*, *354*, 269–279. https://doi.org/10.1098/rstb.1999.0378

Holm, S. (1979). A simple sequentially rejective multiple test procedure. *Scandinavian Journal of Statistics*, *6*, 65–70.

Kleber, J., Chen, Y. C., Michels, B., Saumweber, T., Schleyer, M., Kähne, T., … Gerber, B. (2016). Synapsin is required to 'boost' memory strength for highly salient events. *Learning & Memory*, *23*, 9–20. https://doi.org/10.1101/lm.039685.115

König, C., Khalili, A., Ganesan, M., Nishu, A. P., Gomez, A. P., Niewalda, T., … Yarali, A. (2018). Reinforcement signaling of punishment vs. relief in fruit flies. *Learn Mem*, *25*, 247–257. https://doi.org/10.3389/fnbeh.2010.00189

Li, H. H., Kroll, J. R., Lennox, S. M., Ogundeyi, O., Jeter, J., Depasquale, G., & Truman, J. W. (2014). A GAL4 driver resource for developmental and behavioral studies on the larval CNS of *Drosophila*. *Cell Reports*, *8*, 897–908. https://doi.org/10.1016/j.celrep.2014.06.065

McGuire, S. E., Deshazer, M., & Davis, R. L. (2005). Thirty years of olfactory learning and memory research in *Drosophila melanogaster*. *Progress in Neurobiology*, *76*, 328–347. https://doi.org/10.1016/j.pneurobio.2005.09.003

Malaka, R. (1999). Models of classical conditioning. *B Math O Biologico*, *61*, 33–83.

Michels, B., Saumweber, T., Biernacki, R., Thum, J., Glasgow, R. D. V., Schleyer, M., … Gerber, B. (2017). Pavlovian conditioning of larval *Drosophila*: An illustrated, multilingual, hands-on manual for odor-taste associative learning in maggots. *Frontiers in Behavioral Neuroscience*, *11*, 45. https://doi.org/10.3389/fnbeh.2017.00045

Navratilova, E., Atcherley, C., & Porreca, F. (2015). Brain circuits encoding reward from pain relief. *Trends in Neurosciences*, *38*, 741–750. https://doi.org/10.1016/j.tins.2015.09.003

Niewalda, T., Michels, B., Jungnickel, R., Diegelmann, S., Kleber, J., Kähne, T., & Gerber, B. (2015). Synapsin determines memory strength after punishment- and relief-learning. *The Journal of Neuroscience*, *35*, 7487–7502. https://doi.org/10.1523/JNEUROSCI.4454-14.2015

Paisios, E., Rjosk, A., Pamir, E., & Schleyer, M. (2017). Common microbehavioral 'footprint' of two distinct classes of conditioned aversion. *Learning & Memory*, *24*, 191–198. https://doi.org/10.1101/lm.045062.117

Pauls, D., Selcho, M., Gendre, N., Stocker, R. F., & Thum, A. S. (2010). *Drosophila* larvae establish appetitive olfactory memories via mushroom body neurons of embryonic origin. *The Journal of Neuroscience*, *30*, 10655–10666. https://doi.org/10.1523/JNEUROSCI.1281-10.2010

Pfeiffer, B. D., Ngo, T. T., Hibbard, K. L., Murphy, C., Jenett, A., Truman, J. W., & Rubin, G. M. (2010). Refinement of tools for targeted

gene expression in *Drosophila*. *Genetics*, *186*, 735–755. https://doi.org/10.1534/genetics.110.119917

R Development Core Team. (2016). *A language and environment for statistical computing*. Vienna, Austria: R Foundation for Statistical Computing. http://www.R-project.org

Rohwedder, A., Wenz, N. L., Stehle, B., Huser, A., Yamagata, N., Zlatic, M., … Thum, A. S. (2016). Four individually identified paired dopamine neurons signal reward in larval Drosophila. *Current Biology*, *26*, 661–669. https://doi.org/10.1016/j.cub.2016.01.012

Saumweber, T., Husse, J., & Gerber, B. (2011). Innate attractiveness and associative learnability of odors can be dissociated in larval *Drosophila*. *Chemical Senses*, *36*, 223–235. https://doi.org/10.1093/chemse/bjq128

Saumweber, T., Rohwedder, A., Schleyer, M., Eichler, K., Chen, Y. C., Aso, Y., … Gerber, B. (2018). Functional architecture of reward learning in mushroom body extrinsic neurons of larval *Drosophila*. *Nature Communications*, *9*, 1104. https://doi.org/10.1038/s41467-018-03130-1

Schleyer, M., Saumweber, T., Nahrendorf, W., Fischer, B., von Alpen, D., Pauls, D., … Gerber, B. (2011). A behavior-based circuit model of how outcome expectations organize learned behavior in larval *Drosophila*. *Learning & Memory*, *18*, 639–653. https://doi.org/10.1101/lm.2163411

Schleyer, M., Reid, S. F., Pamir, E., Saumweber, T., Paisios, E., Davies, A., … Louis, M. (2015). The impact of odor-reward memory on chemotaxis in larval *Drosophila*. *Learning & Memory*, *22*, 267–277. https://doi.org/10.1101/lm.037978.114

Schleyer, M., Weiglein, A., Thoener, J., Strauch, M., Hartenstein, V., Kantar Weigelt, M., … Gerber, B. (2020). Identification of dopaminergic neurons that can both establish associative memory and acutely terminate its behavioral expression. *J Neurosci Doi*, *40*, 5990–6006. https://doi.org/10.1523/JNEUROSCI.0290-20.2020

Schroll, C., Riemensperger, T., Bucher, D., Ehmer, J., Völler, T., Erbguth, K., … Fiala, A. (2006). Light-induced activation of distinct modulatory neurons triggers appetitive or aversive learning in Drosophila larvae. *Current Biology 16*, 1741–1747. https://doi.org/10.1016/j.cub.2006.07.023

Selcho, M., Pauls, D., Han, K. A., Stocker, R. F., & Thum, A. S. (2009). The role of dopamine in *Drosophila* larval classical olfactory conditioning. *PLoS One*, *4*, e5897. https://doi.org/10.1371/journal.pone.0005897

Solomon, R. L., & Corbit, J. D. (1974). An opponent-process theory of motivation. *Psychological Review*, *81*, 119–145.

Tanimoto, H., Heisenberg, M., & Gerber, B. (2004). Event timing turns punishment to reward. *Nature*, *430*, 983. https://doi.org/10.1038/430983a

Thane, M., Viswanathan, V., Meyer, T. C., Paisios, E., & Schleyer, M. (2019). Modulations of microbehaviour by associative memory strength in *Drosophila* larvae. *PLoS One*, *14*, e0224154. https://doi.org/10.1371/journal.pone.0224154

Thum, A. S., & Gerber, B. (2019). Connectomics and function of a memory network: The mushroom body of larval Drosophila. *Current Opinion in Neurobiology*, *54*, 146–154. https://doi.org/10.1016/j.conb.2018.10.007

Vogt, K., Yarali, A., & Tanimoto, H. (2015). Reversing stimulus timing in visual conditioning leads to memories with opposite valence in *Drosophila*. *PLoS One*, *10*, e0139797. https://doi.org/10.1371/journal.pone.0139797

Weiglein, A., Gerstner, F., Mancini, N., Schleyer, M., & Gerber, B. (2019). One-trial learning in larval *Drosophila*. *Learning & Memory*, *26*, 109–120. https://doi.org/10.1101/lm.049106.118

Yarali, A., Niewalda, T., Chen, Y. C., Tanimoto, H., Duerrnagel, S., & Gerber, B. (2008). 'Pain relief' learning in fruit flies. *Animal Behaviour*, *76*, 1173–1185. https://doi.org/10.1016/j.anbehav.2008.05.025

Yarali, A., Krischke, M., Michels, B., Saumweber, T., Mueller, M. J., & Gerber, B. (2009). Genetic distortion of the balance between punishment and relief learning in *Drosophila*. *Journal of Neurogenetics*, *23*, 235–247. https://doi.org/10.1080/01677060802441372

Yarali, A., & Gerber, B. (2010). A neurogenetic dissociation between punishment-, reward- and relief learning in *Drosophila*. *Frontiers in Behavioral Neuroscience*, *4*, 1–13. https://doi.org/10.3389/fnbeh.2010.00189

SUPPORTING INFORMATION

Additional supporting information may be found online in the Supporting Information section at the end of this article.

How to cite this article: Weiglein A, Thoener J, Feldbruegge I, et al. Aversive teaching signals from individual dopamine neurons in larval *Drosophila* show qualitative differences in their temporal "fingerprint". *J Comp Neurol*. 2021;529:1553–1570. https://doi.org/10.1002/cne.25037